AN INVESTIGATION INTO PARTIAL DISCHARGE BEHAVIOUR IN IMPULSE AGED POLYMER INSULATION

Makanyane Mosebjadi Caroline Mampane

A dissertation submitted to the Faculty of Engineering, University of the Witwatersrand, Johannesburg in fulfilment of the requirements of the degree of Master of Science in Engineering

Johannesburg, **2012**

DECLARATION

I declare that this research report is my own unaided work. It is being submitted for the Degree of Master of Science to the University of the Witwatersrand, Johannesburg. It has not been submitted before for any degree or examination to any other University.

Candidate Signature :

Name : Makanyane M. Mampane

Date:

ABSTRACT

The objective of this research work is to investigate the behaviour of partial discharges (PD) in impulse aged solid polymer insulation. The investigation was conducted through studying key partial discharge characteristics such as; PDPRP (partial discharge phase resolved patterns), PD magnitude and PD inception voltage in impulse aged and non-aged insulation. Polymer insulation is widely used in electrical equipment such as motors, generators and power cables for high voltage insulation purposes. The insulation can be inevitably exposed to impulse voltages such as lightning. In this work the experimental investigation was performed on underground shielded power cable insulation. Lightning impulses, generated using a single stage impulse generator, were used to age 11 kV, 1 meter cross-linked polyethylene (XLPE) power cable test samples. Artificial cavity defects were then created in each sample. Subsequently, PD tests were performed using the IEC60270 test setup. Similar cavity defects were created in non-aged cable power samples and similar PD tests were conducted for comparative purposes. PD measurements assessed the effect of impulse ageing on PD phase-resolved patterns, PD magnitude and PD inception voltage. The results revealed that PDPRP had a distinct response to impulse ageing and this manifested as distinct changes in PD magnitude peak profiles of positive and negative half cycle patterns. PDPRP of non-aged samples contained a characteristic positive half cycle peak PD magnitude that is smaller than that of negative half cycle peak PD magnitude. The converse applied to the case of aged samples where the PDPRP negative peak magnitude was either larger or equal to the positive peak magnitude. Generally, PD magnitudes of non-aged test samples were larger and varied over a wider range than those in aged samples. PD inception voltage of the aged samples was slightly lower than that of non-aged test samples. The findings on the influence of impulse ageing of insulation on PD characteristics can be interpreted using conventional knowledge on PD mechanisms. These findings can be useful in PD diagnosis technology, for example; during continuous online PD monitoring changes in PD patterns could infer increased exposure of equipment under test to lightning voltage surges.

DEDICATION

I dedicate this work to my future children, may it be a seed to a prosperous future and a beacon of hope that through hard work and persistence great things are possible.

ACKNOWLEDGEMENTS

I would like to thank Professor Ian R. Jandrell, the research leader of the High Voltage Engineering Research group, for his financial assistance and creating research opportunities for me. I would also like to express my gratitude to the National Research Fund (NRF) for their financial contribution towards my research work. I am eternally grateful to Dr Cuthbert Nyamupangedengu for his guidance and unwavering support during the course of my research work. He has given me tremendous support and has been a stellar example of hard work, integrity and good work ethic. My gratitude also goes to the Genmin workshop staff and in particular Mr Harry Fellows, for materials and countless workshop help. Lastly, I would like to thank my friends and most importantly my sisters for their unconditional love and support.

TABLE OF CONTENTS

LIST OF FIGURES

LIST OF SYMBOLS AND ABBREVIATIONS

E_o	Background field
a	cavity radius
b	cavity height
ε_r	Permittivity
p	Pressure
k_s	Surface conductivity
v_o	fundamental photon frequency
Φ	effective detrapping work function
E	electric field inside the void
k	Boltzmann constant
T	temperature
N_{dt}	number of electrons available for being detrapped
t	time elapsed since the last PD event
τ	effective decay time constant
B	dimensionless gas property
E_c	electric stress within the cavity
$\boldsymbol{E}_d$	stress within the insulation
f	dielectric constant
r	radial position of the cavity
R_i	radius of the conductor interface between semiconductor and dielectric
R_o	radius of the dielectric-ground semiconductor interface
K	geometry factor of the enclosed void
Ω	void volume
E_i	applied electric field for the inception of the PD of the streamer type
E_l	limiting applied field for ionization
ε	permittivity of the surrounding insulating material
ε_0	known dielectric constant
$\nabla\lambda_0$	the ratio of the electric field at the position of the void (in absence of the void) to the voltage

between the electrodes (i.e. $\nabla\lambda_0 = {1}/{rIn\frac{R_o}{R_i}}$ for a coaxial arrangement [m^{-1}])

Δ	PD pulse phase shift.
a_{eff}	effective void radius
PD	Partial discharges
PDIV	Partial discharge inception voltage
PDPRP	Partial discharge phase resolved patterns

LIST OF TABLES

1 INTRODUCTION

1.1 Background

An insulator is a non-conducting material that isolates high voltage systems from the surrounding environment. Polymer insulation is widely used in electrical equipment such as power cables, transformers and rotating machines (generators and motors). Polymer insulated power cables have been in use since the 1940s (Hall, 1993). While in service, power cables are exposed to electrical, mechanical and thermal stresses. These stresses in turn instigate changes in the insulation parameters (Grzybowski, Cao, & Shrestha, 2009). The electric stress of interest in this research is the lightning impulse, as it induces typical deleterious stress on insulation due to its high peak voltages and steep rise times. In addition to vulnerability to impulse stress, an intrinsic disadvantage of solid polymer insulation is its susceptibility to partial discharge (PD) induced degradation. PD activity in polymer insulation may eventually lead to complete insulation failure. PD diagnosis is therefore an important insulation condition assessment technique. This research studies the relationship between impulse ageing and PD behaviour in polymer insulation using laboratory based experiments.

1.2 Motivation for the research

If PD defects develop in impulse aged insulation, the following questions arise: Could the behaviour of ensuing PD mechanism be affected by pre-exposure of the insulation to impulse surges? What would be the possible application of such knowledge in PD diagnosis? This research sought to answer these questions through a laboratory-based experimental investigation.

1.3 The dissertation structure

This report presents an experimental study of the behaviour of partial discharges in impulse-aged polymer insulation. It further contributes to knowledge on understanding mechanisms by which impulse surges contribute to ageing of polymer insulation and how this in turn could affect PD activity. The report structure is as follows:

- Chapter 2 presents literature review of PD technology development, the effect of voltage surges on insulation and how knowledge on the relation of the two insulation ageing mechanisms is a crossing link
- Chapter 3 presents detailed theory on cavity PD mechanism in the context of how impulse ageing could affect PD phase resolved patterns, PD magnitude and PD inception
- Chapter 4 presents design processes used in setting up the laboratory experiments
- Chapter 5 presents the experimental work procedures performed in order to investigate the behaviour of PDs in impulse aged insulation
- Chapter 6 presents the experimental findings, analysis and discussion
- Chapter 7 concludes the report and gives recommendations for future work
- Chapter 8 is the appendix

1.4 Conclusion and pointers to the next chapter

This chapter presented background information, motivation of the research objective, key findings of the research and a layout of the dissertation structure. The next chapter presents a literature survey of PD research history and development; and impulse ageing of insulation.

2 PARTIAL DISCHARGES AND IMPULSE AGED INSULATION

PD research has evolved and advanced significantly over the past eight decades (Bartnikas, 2002). Researchers are currently exploring other mechanisms that could affect PD behaviour in polymer insulation. Currently, the effect of surge impulses on PDs is an emerging research area. This chapter reviews the advancement of PD research; followed by a discussion on current knowledge of impulse ageing on insulation. The knowledge on the effect of impulse ageing on PD behaviour in polymer insulation is identified as the missing link. This chapter concludes with a presentation of the research objective and methodology.

2.1 Problem statement

Partial discharges are defined as localized small electric sparks or discharges. The discharges do not

bridge the insulation between conductors (IEEE Power Engineering Society, 2006). They occur in defects in the insulation, or at interfaces, between insulating materials or surfaces, or between a conductor and a floating metal component (not connected electrically to the high voltage conductor nor to the ground conductor) or between floating metal components (IEEE Power Engineering Society, 2006). PD defects can develop in insulation due to various reasons. They may be a consequence of insulation condition deterioration or improper installation, faulty design or poor workmanship (in the case of cable joints and terminations). PDs are essential phenomenon used in high voltage insulation condition assessment. PD measurements are used in insulation diagnosis to check the reliability of insulation systems, classify insulation defects, and evaluate failure threats and to show the condition status of equipment (Niemeyer, 1995), (Kelen, 1995).

PD diagnosis has been an essential part of high voltage research since the early 1940's and has spanned over decades (Nattrass, 1993). Early research focused on the mechanism of cavity PD behaviour in polymer insulation. The cavity defect PD process consists of: PD inception, physiochemical processes, electrical treeing and eventual insulation breakdown (Devins, 1984). Remarkable progress has been achieved in the understanding of cavity PD mechanisms; consequently PD diagnosis practitioners now possess widely accepted knowledge (Crichton, Karlsson, & Pederson, 1989). PD research has since expanded to enhancing PD detection, classification and location techniques.

It is now common knowledge that PDs evolve during the PD ageing process in polymer insulation. Different PD regimes are characterized by pulse shape, rise time, fall time, peak magnitude, light intensity and order of magnitude (Morshuis, 1995). Over the years, there has been varying progress regarding types of PD detection equipment and behavioural aspects being examined (Gulski, Morshuis, & Kreuger, 1994). Most of the knowledge on PD mechanisms in polymer insulation has been generated through equipment using sinusoidal voltages. The same however, does not hold for partial discharge mechanisms in polymer insulation under impulse voltages (Bartnikas, 2002), (Lindell, Bengtsson, Blennow, & Gubanski, 2008).

An impulse voltage is a unidirectional voltage that rises rapidly to a peak value and decays relatively slowly to zero (Kreuger, 1989). There are generally two types of standardized impulse voltages, namely; lightning and switching over-voltages. Lightning discharges and switching impulses may create travelling overvoltage surges in electrical equipment. Switching impulses are at all times related to

equipment operating voltage and the waveform shape is influenced by the impedances of the system as well as the switching conditions (Kreuger, 1989).

The effect of overvoltage surges on high voltage equipment insulation is an active area of research. The U_{50} test is also used to check the breakdown stress/strength of insulation under test (Kuffel, Zaengl, & Kuffel, 2000). The effect of impulse voltages on important properties of insulation such as dielectric strength, space charge and tan-delta has also been investigated (Berstein, 2012). Impulse voltages alter certain insulation characteristics and PD diagnosis of insulation is used to check the condition of the insulation. It is therefore hypothesized that PD behaviour in impulse-aged insulation could be different from that in un-aged insulation. Research into this area is generally still in its infancy.

In this research, experimental investigations were performed in this regard under conditions where power cable insulation was subjected to lightning impulses. Afterwards PD tests followed to check the effect of lightning impulses on PD characteristics. The characteristics are PD magnitude; inception voltage; and PDPRP (phase resolved patterns). These characteristics are important as they contain and reveal useful information about cavity PD mechanism.

2.2 The ageing of insulation through impulses

Insulation material is characterized using parameters such as tan-delta (dielectric loss), dielectric strength and permittivity. Insulation integrity can be defined using these characteristics. For example, cross-linked polyethylene (XLPE) is widely used in power cable insulators due to its inherent, high dielectric strength, low permittivity and tan delta values. These limit reactive currents and dissipation losses respectively (Berstein, 2012).

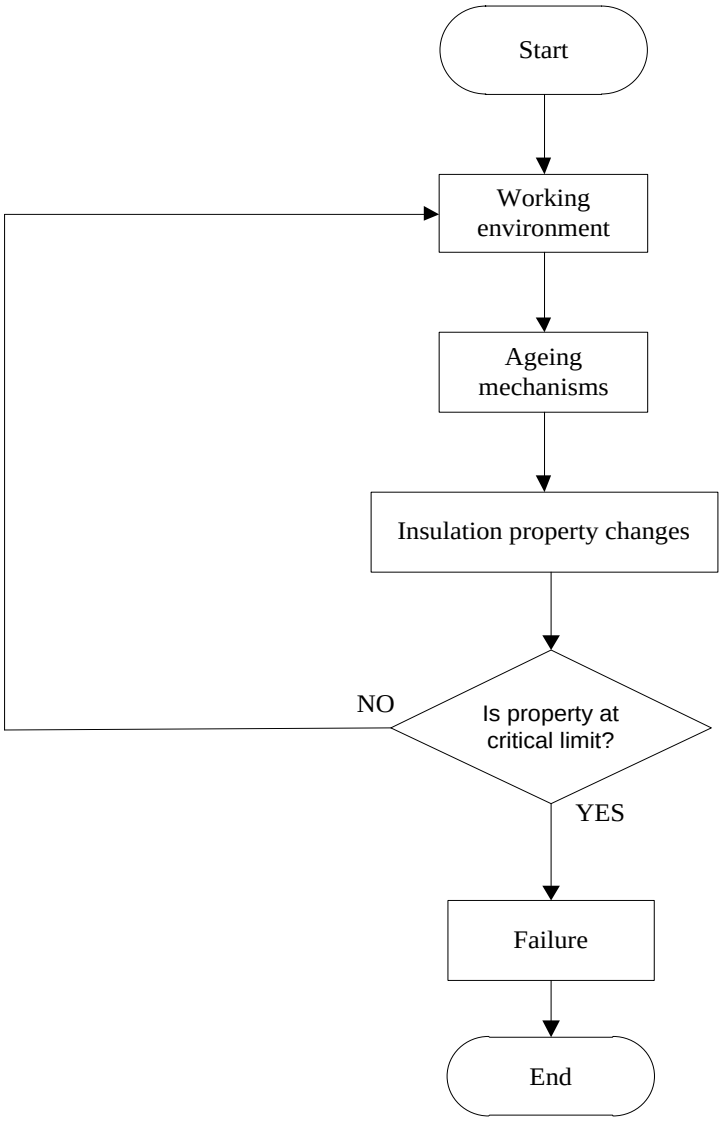

Figure 2-1: A flowchart depicting an insulation failure process (Bahaardoorsigh & Rowland, 2005)

Figure 2-1 is an insulation failure flowchart and illustrates how a change in an insulation parameter, for example dielectric strength, might lead to failure if it is at a critical limit (Bahaardoorsigh & Rowland, 2005).

Literature indicates that the following electrical parameters respond to impulse damage of polymeric insulation, namely; dielectric loss, dielectric strength, space charge and insulation capacitance. PD diagnostics is used to assess insulation integrity. As a result, researchers are now interested in how impulse ageing affects PD behaviour and the implications of this knowledge on field application of PD

diagnosis technology. The knowledge of insulation ageing by impulse surges is still not well established, even though research has been conducted in this area (Dao, Lewin, & Swingler, 2009).

The mechanisms of impulse ageing within insulation can be classified into physical and electrical effects; and these are mutually related. The impact of lightning impulses on insulation often manifests as surface flashovers. The physical signs of impulse damage on insulation ranges from minor to substantial erosion, with burn marks included (Mason, Wilson, Given, & Fouracre, April 2008). These roughen the insulation texture and distort the uniformity of the surrounding electric field and in turn have implications on breakdown characteristics. Outcomes from experimental tests on PE (polyethylene) cables showed that AC and impulse breakdown values may not be considerably altered due to exposure to periodic surges (Murata, Katakai, & Kanaoka, 1996), (Hartlein, Harper, & Ng, 1989).This however, is on condition that the AC voltage stress magnitude is not sufficiently large to affect breakdown (Bahaardoorsigh & Rowland, 2005). According to (Hartlein, Harper, & Ng, 1989) a high surge magnitude decreases cable life.

(Grzybowski, 2007) used PD parameters such as PD phase resolved patterns, apparent charge and AC breakdown voltage to evaluate the effect of 5000 standard switching impulses on 1 meter 15 kV XLPE cable segments at defined intervals. Measurement results showed no evident indication of insulation ageing in the cables after 1000 switching impulses were applied. After 4500 impulses, PD repetition rate increased on the negative half cycle of measured PD phase resolved patterns and was a signal that insulation deterioration had occurred. Apparent charge magnitude profiles displayed a solid declining trend with impulse ageing. The AC breakdown voltage of the XLPE cable was reduced considerably by 5000 impulses. The change in these parameters was attributed to insulation deterioration (Grzybowski, 2007) .

Dao et al (2009) studied the effect of lightning impulses on the dielectric properties of HDPE (high density polyethylene). Three thousand lightning impulses were applied on 5 mm deep by 30 mm long moulded HDPE samples. Results showed that the breakdown strength of the HDPE insulation material was decreased considerably by at least 20% after exposure to 3000 impulses. This is assumed to be caused by lightning impulses generating excited electrons with high energy that penetrate the bulk dielectric. These electrons can cause bond scission and create charge trapping centres. The traps enhance charge build up and alter the breakdown strength of the sample. Alternately, the space charge may only be present in the vicinity of the surface of the sample and may dissipate overtime. At times the

lightning impulse may only provide thermal energy that elevates the sample temperature (Yilmaz, Oztas, & Kalenderi, 1995) (Dao, Lewin, & Swingler, 2009). The results also revealed that the dielectric tan-delta and the real part of the relative permittivity increased with impulse ageing.

Furthermore, dielectric relaxation and space charge measurements showed that aged samples have increased conduction losses than non-aged samples and that the insulation space charge profile was altered by impulse ageing. Increased conduction losses imply that the aged insulating material experiences increased temperatures when subjected to the same electrical stress as un-aged insulation material (Dao, Lewin, & Swingler, 2009). The reduced electric field strength of the HDPE insulation after sustained exposure to impulse voltages increases conductivity and space charge retention of the insulation material (Dao, Lewin, & Swingler, 2009).

Sun et al (2009) studied PD under AC, DC and impulse voltage on a needle-plate in air arrangement. The rise time and fall time of the impulse waveform were 1.25/48 μs. Generally, PDs under impulse voltages took place on the rising portion of the impulse wave (Densley & Salvage, 1971) and had a broader frequency range than PDs under AC (alternating current) or DC (direct current) voltage. This was attributed to PD frequency aliasing with the impulse voltage frequency. PDs under impulse voltage were more irregular and indeterminate than PDs under AC (alternating current) or DC (direct current) voltage. This was concluded after a series of experiments revealed a statistical pattern of PDs under impulse voltages.

Hartlein et al (1989) studied the effects of voltage surges on extruded dielectric cable life. 15kV XLPE cables were exposed to 40 kV, 70 kV and 120 kV lightning impulses. Experimental results revealed that lightning voltage impulses may decrease power cable operating lifetime and lightning impulse voltage magnitude does not influence cable failure rates significantly. The effect of impulse ageing on polymer insulation is an interesting phenomena and brings about the objective of this research presented in the following section.

2.3 Research objective

The objective of this research is to investigate the effect of lightning impulses on PD behaviour in medium voltage (MV) power cable polymer insulation. Power cable insulation may develop defects that give rise to PD activity. The following insulation degradation induced by PDs depends on the electrical

properties of the insulation. Impulse ageing of insulation affects the electrical properties of insulation. It follows therefore that PD characteristics could be influenced by impulse surges. The research aims at investigating PD behaviours in impulse aged polymer insulation and seeks to address the following question:

- How are PD characteristics affected by impulse ageing of polymer insulation?

2.4 Overview of the investigation methodology

The study method involved literature review on PD mechanisms to establish current knowledge on PD behaviour in impulse aged insulation and related work. The knowledge was then used to design and execute the experimental work. This was achieved by preparation of power cable test samples for testing, followed by subjecting half of the samples to lightning impulses and lastly PD tests were performed on all the samples for comparative purposes.

2.5 Conclusions and pointers to the next chapter

PD diagnosis technology research has been active and progressive since early 1940's. The research has evolved and currently includes understanding PD behaviour in impulse aged insulation. The phenomenon can be studied through analysing the relationship between PD characteristics and impulse ageing of insulation. The next chapter presents these PD parameters and theoretically predicts how they can be affected by impulse ageing.

3 CAVITY PARTIAL DISCHARGES: A REVIEW OF THE THEORY

The partial discharge phenomena is fairly complex and it is best described by its inherent characteristics. These include PD inception voltage, recurrence rate; apparent charge magnitude and phase resolved patterns. PDs are a result of insulation breakdown either due to an electric field enhancement inside the insulation or on the insulation surface (Kreuger, 1989). This chapter presents cavity defect parameters and PD characteristics in detail and speculates on how the latter can be influenced by impulse ageing of polymer insulation.

3.1 Types of PD

Various PD types are illustrated in Figure 3-1.

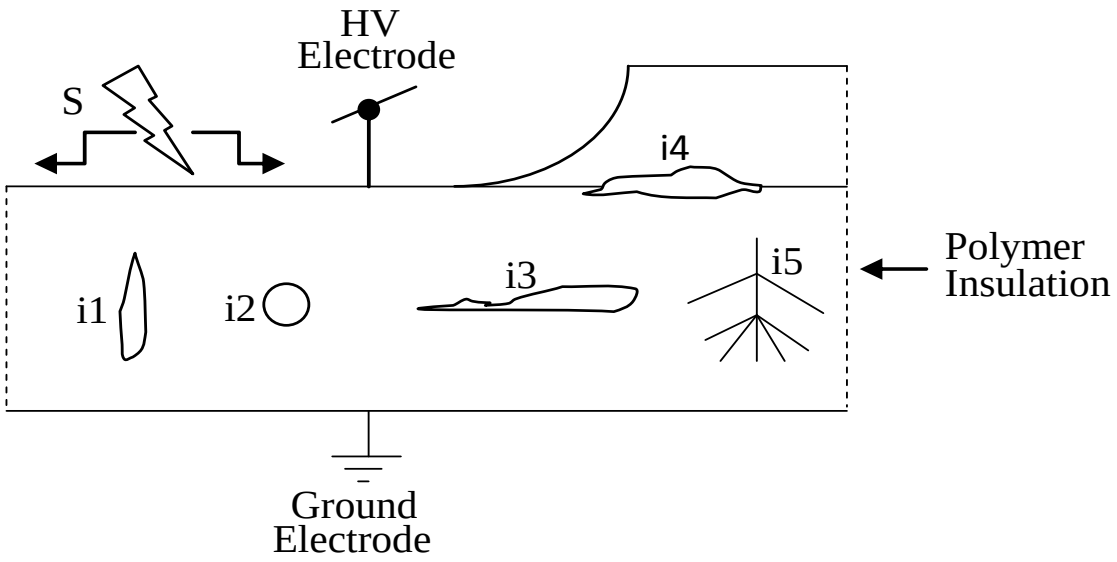

i1 long vertical cavity
i2 spherical cavity
i3 flat cavity
i4 longitudinal cavity
i5 electrical tree
S surface discharge

Figure 3-1: Types of PD

S is a surface discharge, i1 to i5 are internal PD sources. The origin of internal discharges may be gas voids, or foreign intrusions into the insulation. Spherical cavities are usually formed when gas bubbles are trapped during insulation curing. Longitudinal cavities may be formed at interfaces of two insulation

surfaces. Electrical trees are the final stages of partial discharge progression prior to insulation breakdown. Surface discharges are caused by stress factors parallel to an insulation surface such as lightning voltage surges. Among possible defects in this work only cavity discharges were studied as they are the most dangerous and their mechanisms are now generally well understood (Morshuis, 2005). The next section presents geometrical parameters of gas void that influence PD behaviour.

3.2 PD defect geometrical parameters

In power cables gas bubbles are trapped within the insulation, as a result of poor workmanship during the assembly of cable terminations and joints. Although rare, gas bubbles can also be trapped in the main cable insulation during the manufacturing process. The parameters of an insulation cavity that influence PD mechanisms are given in Table 3-1 (Niemeyer, 1995).

Table 3-1: Generalized gas void parameters and their control factors (Niemeyer, 1995)

Category	Parameter	Symbol
Geometry	Background field	E_o
	Defect dimensions	b and a
Bulk Materials	Permittivity	ε_r
	Pressure	p
	Gas ionization	$(E/p)_cr$, B, η, γ
Cavity Surface	Electron emission	Φ, $\dot{\tau}_{dt}$
	Surface conductivity	k_s

The cavity geometrical parameters can be categorized into; geometry, bulk materials and cavity surface. The first category pertains to the depth (b) and radius (a) in the direction of the surrounding field (E_o) and vertical to it respectively. The second category is the bulk attributes of the insulation and gaseous substances trapped in the PD activity. These consist of the relative permittivity ε_r of the solid dielectric, the type of gas and corresponding pressure p, and the parameters $(E/p)_{cr}$, B, n, γ which integrally represent the ionization characteristics of the gas or gas-insulation surface interface. $(E/p)_{cr}$ is the pressure reduced critical field, B is a gas property, η is the electron attachment co-efficient of the gas and γ is a dimensionless proportionality factor. The cavity surface category of parameters pertains to cavity surface boundary conditions that are involved in PD activity. The cavity surface conditions influence the variations of the gas ionization features by surface contributions, charge and electron release from surfaces and charge motion along surfaces (Fruth & Niemeyer, 1992).

3.3 The recurrence of partial discharges

The recurrence of PD activity is depicted in Figure 3-2. An ideal cavity enclosed within polymer insulation subjected to a sinusoidal wave voltage is assumed. When a free electron is available and the voltage across the cavity attains its Paschen breakdown value (E_{inc+} or E_{inc-}), a PD will occur. As a result, the voltage across the cavity will decrease rapidly either to zero or to a residual value. The PD appears as a pulse superimposed on the power frequency voltage sine wave. Subsequent to PD extinction, the voltage across the cavity rises again until it attains a new breakdown value and a follow up PD takes place. This process repeats many times on the rising and falling regions of the applied voltage as illustrated in Figure 3-2. The resulting PD pulses exhibit stochastic behaviour characterized by intermittency and rapid fluctuations. This is caused by randomness in the time it takes a PD initiating electron to be available (statistical time lag) (Bartnikas, 2002). Scarce initial electrons result in a high PD inception voltage and PD magnitude and these shape the resultant PD phase resolved pattern (PDPRP).

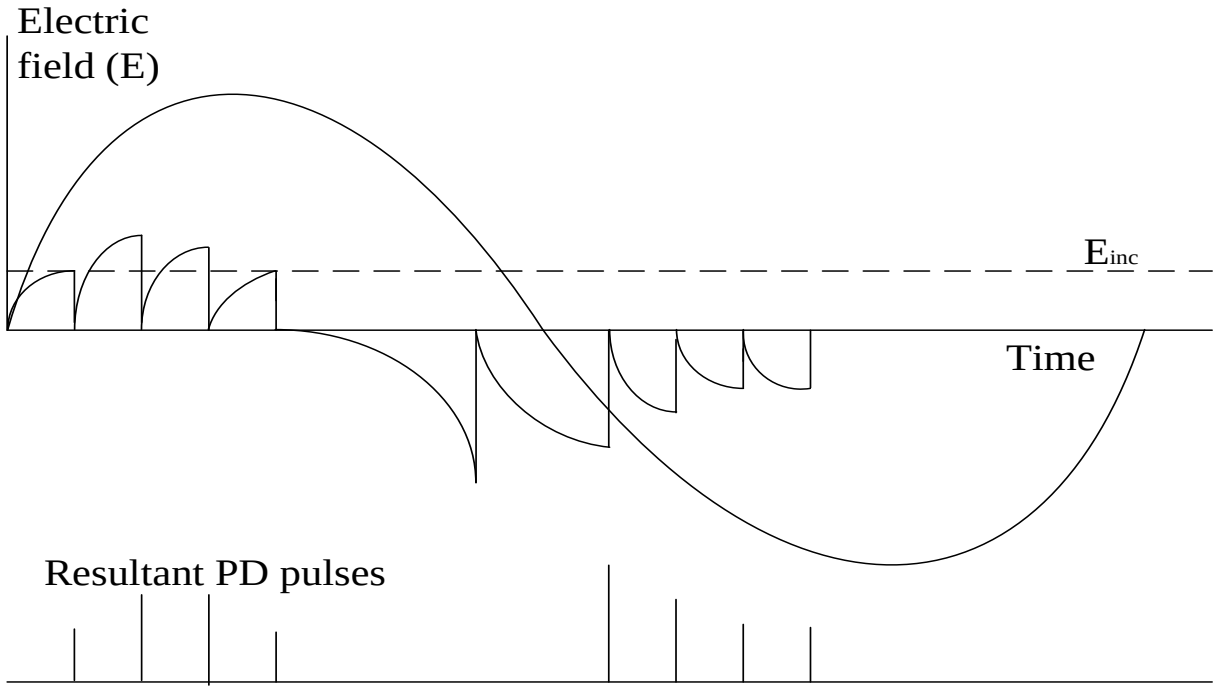

Figure 3-2: The recurrence of PDs (Fruth& Niemeyer, 1992)

The subsequent sections discuss the theoretical models of the following PD characteristics: PD inception voltage, PD magnitude and PD phase resolved patterns and how these characteristics respond to impulse ageing of insulation.

3.4 PD inception voltage and how it can be influenced by impulse ageing

In order for PD activity to occur, two pre-requisites must be fulfilled, namely, an initial electron must be present to start an ionization avalanche and the field (E) in the void must exceed the discharge inception voltage (E_{inc}). The initial electron is the main cause of the statistical characteristics of the PD process such as inception delay, frequency of occurrence and phase distribution. Initial electrons are generated by two processes; volume and surface processes. Volume generation processes are driven by radiated gas ionization due to energetic photons and field detachment from negative ions. Surface processes include the production of electrons from cavity surfaces where they have been trapped in preceding discharge events (Niemeyer, 1995). In the initial stages of PD activity, the statistical time lag is long as a result of the existence of electronegative oxygen and the release of few electrons from the insulation surface due to the high ionization potential of the un-aged dielectric (~10eV for polyethylene). Hence in this case PD initiates at over-voltages of approximately 30% causing a transient development of the avalanche process (Morshuis, 1995).

Additional startup electrons may be generated by surface release from the void layer if the work function is sufficiently low. The leading electron generating process depends on properties of the insulating material and the condition of the cavity layer. Electron generation from a void layer is minimal in smooth and pure polymer insulation due to its high work function. The same applies under bulk electron ionization conditions, as the passage of electrons produced into the insulation is small; hence the diffusion depth into the void is also very small.

After a PD event, surplus electrons are available from charges deposited on the void layer. The rate ($\dot{N}_{dt}$) at which first electrons are produced from the void layer is expressed as in Equation 3.1 (Niemeyer, 1995):

$$\dot{N}_{dt} = N_{dt} v_o exp - \frac{\Phi - \sqrt{(eE/(4\pi\varepsilon_o))}}{kT} \tag{3.1}$$

Where:

- v_o is the fundamental photon frequency [s^{-1}]
- Φ is an effective detrapping work function [eV]

E is the electric field inside the void [V/m]

k is the Boltzmann constant [J/K]

T is the temperature [K]

N_{dt} is the number of electrons available for being detrapped

N_{dt} is governed by a production and decay equilibrium. Charges are produced during a discharge and charge decay occurs in the time interval between successive PD events. The number of detrappable electrons is expressed as in Equation 3.2 (Niemeyer, 1995):

$$N_{dt} = \xi \left(\frac{q}{e}\right) \tag{3.2}$$

Where:

$\xi < 1$ is a proportionality factor which describes the fraction of the charge carriers which results in the creation of detrappable electrons [dimensionless]

(q/e) is the elementary charge [dimensionless]

During PD activity the number of detrappable layer electrons is reduced by scattering inside the insulation. These losses make N_{dt} to be a function of time as in Equation 3.3 (Niemeyer, 1995):

$$N_{dt}(t) = \xi \left(\frac{q}{e}\right) \exp\left[-\frac{t}{\tau}\right] \tag{3.3}$$

Where:

t is the time elapsed since the last PD event [s]

τ is an effective decay time constant [s]

The variables of interest in Equation 3.1 are N_{dt} and Φ .The cavity surface work function Φ is defined as the ability of a material to release electrons. Impulse ageing of insulation injects electrons into the insulation. This in turn lowers the insulation work function (Φ) and augments the number of detrappable electrons (N_{dt}). As a result, the rate at which initial electrons are produced from the void layer ($\dot{N}_{dt}$) during a PD event is increased. An abundance of seed electrons reduces the statistical time lag and thus

lowers the PD inception voltage. It is therefore postulated that the inception voltage will be reduced by impulse ageing of polymer insulation. Once an electron has been detrapped and available for a PD event, a stress condition has to be fulfilled and this is called the streamer criterion. The former is fulfilled if the electric stress in the cavity equals or exceeds the streamer inception stress level as shown in Equation 3.4 (Niemeyer, 1995):

$$E_{inc} = E_{str} = E\left[1 + \frac{B}{\sqrt{2ap}}\right] \tag{3.4}$$

Where:

- B is a constant and gas property [Pa.m]
- p is the gas pressure [Pa]
- a is the cavity radius [m]

In a gas void enclosed in insulation, the stress in the void is a function of the stress in the remainder of the insulation. The stress within the void is enhanced and if it is higher than the Paschen breakdown strength of air, a PD is initiated.

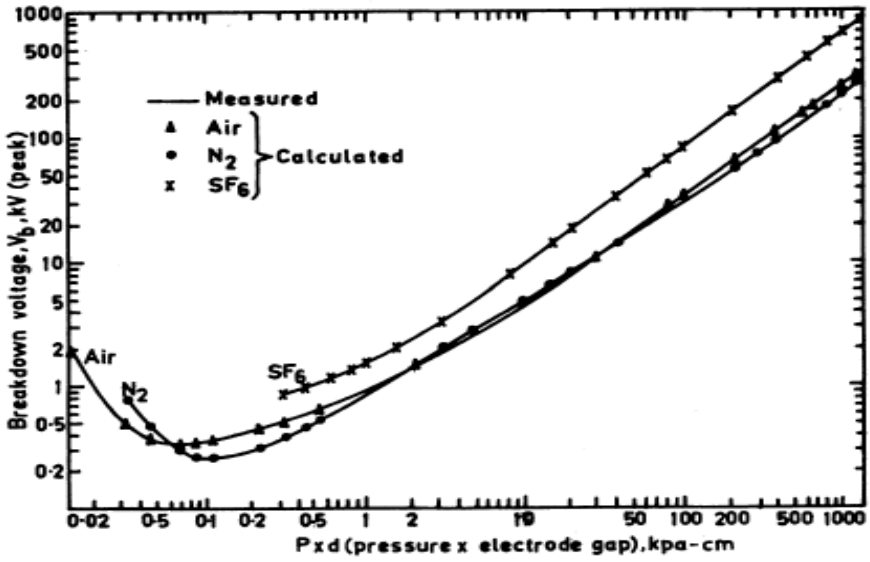

Figure 3-3: Paschen curves for air, Nitrogen and Sulphur Hexafluoride (Husain & Nema, 1982)

The gas type, cavity pressure and discharge gap size significantly affect the breakdown strength of the cavity. This relationship is governed by the Paschen curve as illustrated in Figure 3-3. The Paschen

curve shows that breakdown voltage of a gap is a function of gap distance multiplied by gas density, thus there are distinct Paschen curves for different gases.

The electric field enhancement that occurs within a void is defined by a factor which varies with cavity dimensions, location and geometry of electrodes fitting in the insulation. The electric field enhancement factor is expressed as in Equation 3.5 (Kreuger, 1989):

$$f = E_c/E_d \tag{3.5}$$

Where:

- f is the electric field enhancement factor [dimensionless]
- E_c is the electric stress within the cavity [V/m]
- $\boldsymbol{E}_d$ is the stress within the insulation [V/m]

For a spherical void in insulation between parallel plate electrodes, the electrical stress enhancement is as expressed in Equation 3.6 (Kreuger, 1989):

$$f = 3\varepsilon_r/(1 + 2\varepsilon_r) \tag{3.6}$$

Where:

- f is a dielectric constant [dimensionless]

The PD inception voltage (V_c) is the voltage on the electrodes at the instant of discharge pulse occurrence (Gulski, 1995). In a coaxial cable the PD inception voltage was derived and expressed as in Equation 3.7 (Chan, Duffy, Hiivala, & Wasik, 1991):

$$V_c = 24.2p\left\{rIn\frac{R_o}{R_i}\right\}\left\{\frac{2\varepsilon_r+1}{3\varepsilon_r}\right\}\{\frac{8.6}{\sqrt{2ap}} + 1\} \tag{3.7}$$

Where:

- p is the pressure of the air within the cavity [Pa]
- r is the radial position of the cavity [m]

R_i is the radius of the conductor interface between semiconductor and dielectric[m]

R_o is the radius of the dielectric-ground semiconductor interface [m]

a is the radius of the cavity [m]

ε_r is the relative permittivity of the insulation [dimensionless]

Literature shows that impulses alter the dielectric properties of insulation such as relative permittivity (ε_r) (Dao, Lewin, & Swingler, 2009). PD inception voltage of a cavity in cable insulation is a function of the relative permittivity as shown in Equation 3.7. If other parameters are held constant, Figure 3-4 illustrates the relationship between PD inception and relative permittivity using Equation 3.7. The relative permittivity parameter (ε_r) is an essential component when investigating the effect of impulse voltage on PD inception voltage. It is postulated that the effect of impulse voltage surges on insulation also causes PD inception voltage to change and this was practically verified as presented later in this dissertation. It is important to note that Equation 3.7 holds under initial conditions only. Subsequent discharge mechanisms may influence some of the parameters in Equation 3.7 for example pressure (p).

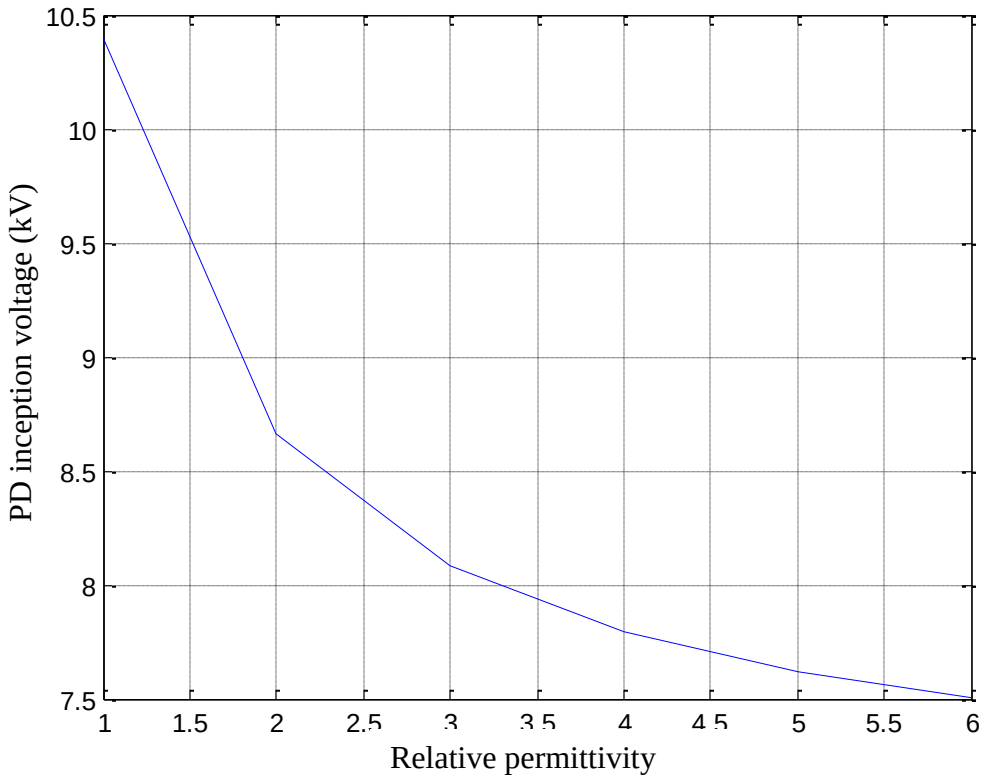

Figure 3-4: A plot showing the relationship between PD inception and relative permittivity

The following section discusses PD magnitude in the context of how it could be influenced by impulse

ageing.

3.5 PD Magnitude and how it can be influenced by impulse ageing of the insulation

PD magnitude is the amount of charge in picocoulomb transferred during a discharge pulse. PD magnitude changes with PD progression in insulation and consequently it is used to classify PD ageing stages. It is also used in practice to evaluate PD in HV constructions and to derive and describe other PD characteristics such as PD energy and PD phase resolved patterns (Gulski, 1995).

Prior to a PD event, the field inside the insulation surrounding a cavity defect is E_o as depicted in Figure 3-5. The field inside the cavity is intensified by an electric field enhancement factor f and results in a cavity field of fE_o. Once the streamer criterion is fulfilled and a PD initiating electron is available, a PD event occurs. This deposits a dipole charge on the walls of the cavity as shown in Figure 3-5 (b). The charge deposit creates a field E_q inside the cavity that opposes fE_o and results in a residual stress E_{res}.

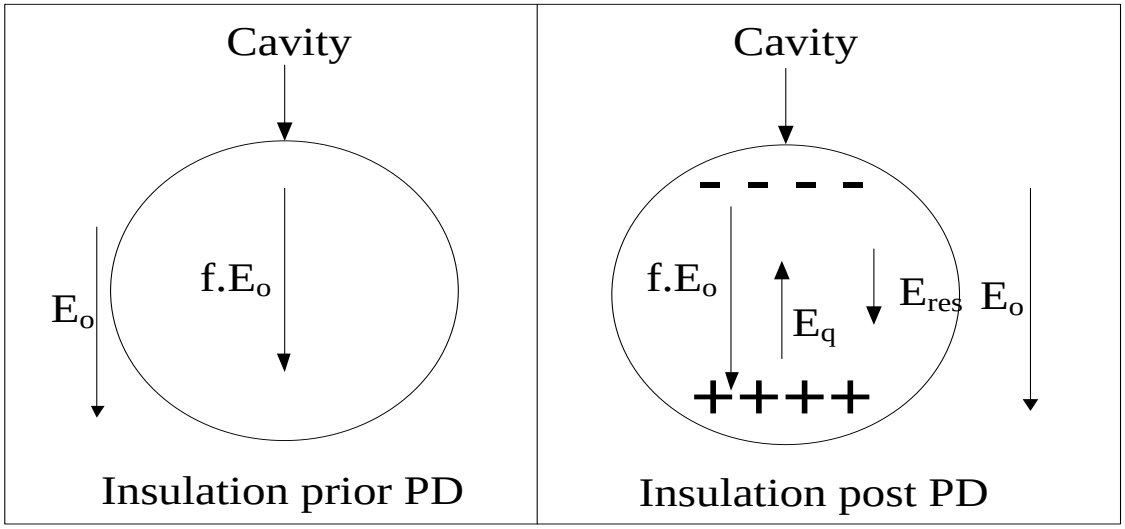

Figure 3-5: Charge deposit on void walls prior to and post PD and corresponding electric field (Gutfleisch & Niemeyer, 1995)

After a PD event the charge induced at the measuring electrode (apparent charge) is the PD magnitude and it is given by Equation 3.8 (Danikas & Adamis, 1997):

$$q = K\varepsilon\varepsilon_0(E_i - E_l)\Omega\nabla\lambda_0 \tag{3.8}$$

Where:

- K is the geometry factor of the enclosed void [dimensionless]
- Ω is the void volume [m^3]
- E_i is the applied electric field for the inception of the PD of the streamer type [V/m]
- E_l is the limiting applied field for ionization [V/m]
- ε is the permittivity of the surrounding insulating material [dimensionless]
- ε_0 is the known dielectric constant [F/m]
- $\nabla\lambda_0$ gives the ratio of the electric field at the position of the void (in absence of the void) to the voltage between the electrodes (i.e. $\nabla\lambda_0 = {}^{1}\!/_{rIn\frac{R_o}{R_i}}$ for a coaxial arrangement [m^{-1}])

Equation 3.8 is commonly referred to as Pedersen's model (Crichton, Karlsson, & Pederson, 1989). It is derived from the streamer criterion. The field difference $E_i - E_l$ is expressed as Equation 3.9:

$$E_i - E_l = 1 + \frac{B}{\sqrt{2ap}} \tag{3.9}$$

Where:

- B is a constant and gas property [Pa.m]
- p is the gas pressure [Pa]
- a is the cavity radius [m]

Substituting Equation 3.9 in Equation 3.8 is the apparent charge of a cavity in a coaxial cable as expressed in Equation 3.10 (Danikas & Adamis, 1997):

$$q = K\varepsilon\varepsilon_0 \left\{ \left(1 + \frac{B}{\sqrt{2ap}}\right) \Omega \; X \left({}^{1}\!/_{rIn\frac{R_o}{R_i}} \right) \right\} \tag{3.10}$$

As in PD inception, the permittivity (ε) is a key parameter in the expression of PD apparent charge. Changes in insulation permittivity caused by impulse ageing of the insulation may result in changes in

PD magnitude. The former is expected to conform to PD theory and reduce with insulation ageing. The following section discusses PD phase resolved patterns in the context of how they could be influenced by impulse ageing of the insulation.

3.6 PD phase resolved patterns: how they can be affected by impulse ageing of insulation

PD phase resolved patterns are PD magnitude distributions on the power frequency cycle as a function of phase angle. PD phase resolved patterns are used in practice to do the following: analyse PD pulse repetition in each half cycle, detect PD defect type and assess PD conditions (Gulski, 1995). PDPRPs are a widely used tool in characterization of partial discharges (Fruth & Niemeyer, 1992). PD initiating electrons are responsible for the statistical time lag and PD magnitude. Collectively with the charge deposited on the cavity surface after a PD event, they regulate the qualitative and quantitative features of the random PD phase resolved pattern.

There are two types of PD phase resolved patterns depending on the availability of PD initiating electrons, namely; regularly structured patterns and random patterns. When there is a large quantity of electrons PD pulses immediately take place when the electric field in the cavity is greater than the inception field E_{inc}. The statistical time lag is negligible and consequently the PD pulse pattern is steady. The corresponding PD magnitude q_{min} is equivalent to the minimal charge. The minimal charge q_{min} is generated by a PD event if the applied field E is equivalent to the streamer inception field E_{str}, and an initial electron is present. The maximum charge q_{max} is obtained after a discharge has occurred at the maximum of the applied voltage that gives E_{max}. When initial electrons are scarce, PD pulses are intermittent and as a result of deficient electrons, will appear when the applied field E exceeds the inception field. Therefore, the corresponding charge magnitudes vary between q_{min} and q_{max}. Δ is a phase shift between PD pulses.

The relationship between PDPRP and impulse ageing of insulation is of interest in PD diagnosis technology. With reference to PD mechanism as illustrated in Figure 3-6, if the number of initial electrons is changed due to impulse ageing, the PD magnitude and the repetition rate of pulses in each half-cycle will change, consequently the PPRPD will also be affected. In this work, practical tests were performed to verify the relationship.

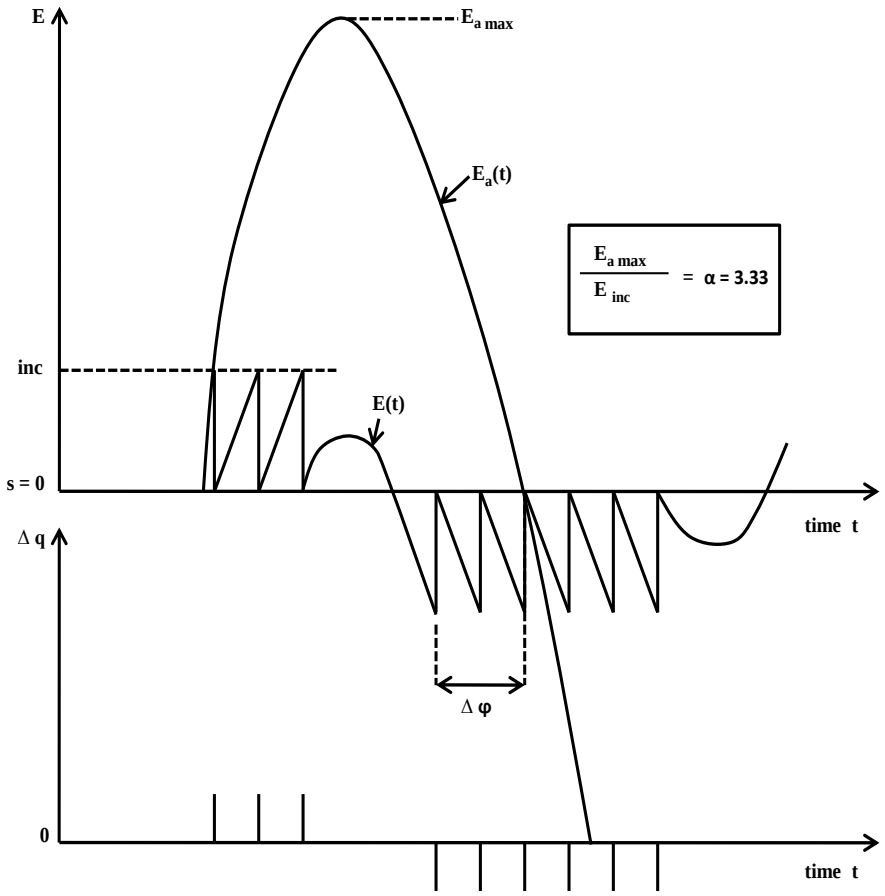

Figure 3-6: A regular PD phase resolved pattern

3.7 Conclusions and pointers to the next chapter

In this chapter PD types, cavity defect geometries, PD inception, PD Magnitude and PD phase resolved patterns were presented. The effect of impulse ageing on these PD characteristics was reviewed. The next chapters present the experimental tasks and tests performed to verify these predictions.

4 EXPERIMENTATION SYSTEM PREPARATION AND DEVELOPMENT

In the previous chapters analytical models of PD inception voltage, PD magnitude and PD phase resolved patterns were analysed in the quest of interpreting how these characteristics could be affected by impulse ageing. In this chapter the research method and single stage impulse generator circuit operating mechanism are presented. The procedure followed in preparing the XLPE cable segments for testing and PD test circuit calibration and operating philosophy are also presented.

4.1 The experimental method

Two sets of new 11 kV, Aluminium core XLPE power cable test samples were prepared for the main experiments. Each set consisted of six, epoxy resin terminated, 1 meter power cable segments. Using a single stage impulse generator, one set of the samples was repetitively subjected to 5000 standard lightning impulses (an example of such impulse voltage waveform is illustrated in Figure 4-1 in parallel).

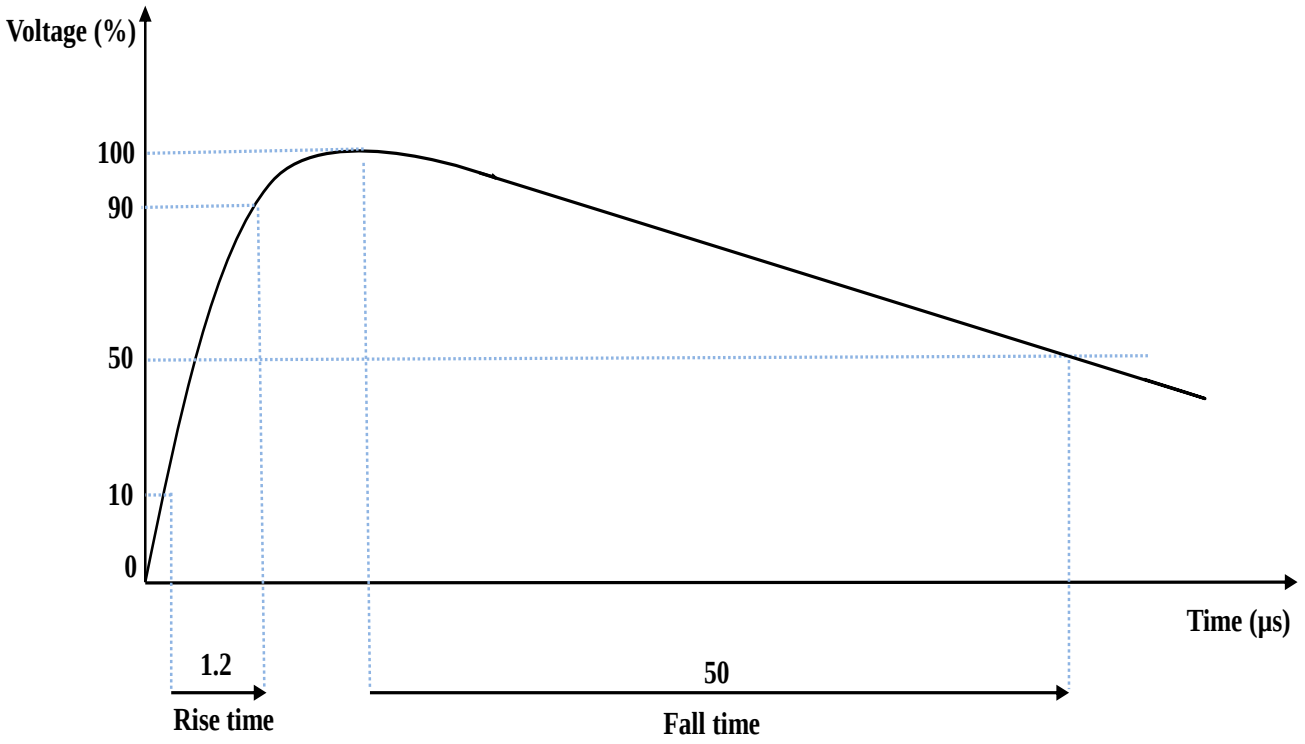

Figure 4-1: A full lightning impulse waveform (Swafield, Lewin, Dao, & Hallstroom, 2007)

These are the test specimens termed impulse-aged power cable test samples in the rest of this report. Artificial cylindrical defects of 3 mm diameter and 1mm depth were created in both the impulse-aged and un-aged power cable test samples. PD measurements were then performed on both sample sets using a 50 Hz AC supply voltage in accordance with the IEC 60270 standard PD testing method. The PD characteristics of the un-aged and impulse-aged power cable test samples were then analysed and evaluated.

4.2 Impulse generator circuit

The power cable test samples were aged using a single stage impulse generator of which the equivalent circuit is shown in Figure 4-2. V_{in} supplies AC voltage to the diode bank (D). The former rectifies the AC input voltage (V_{in}) and supplies the impulse shaping circuit with DC voltage. C1 charges the impulse shaping circuit with DC voltage through resistor R1. The air gap (G) acts as a voltage switch that operates the single generator circuit and C2 discharges the impulse shaping circuit through resistor R2. Collectively R1, C2 and R2 form the lightning impulse wave shaping network. R1 damps the single generator circuit and controls the front time. R2 discharges capacitors C1 and C2 and essentially controls the wave tail (Kuffel, Zaengl, & Kuffel, 2000). DUT (device under test) represents a full load that consist of six power cable test samples connected in parallel.

Figure 4-3 shows the actual measured lightning impulse output waveform of the single stage generator circuit that was recorded using a digital Tektronix oscilloscope. The impulse rise times was measured as 1.08 µs while the fall time was 48.53 µs. The fall and rise times were within the ± 30% tolerance margin of the IEC 60060-1 standard 1.2/50 µs lightning impulse.

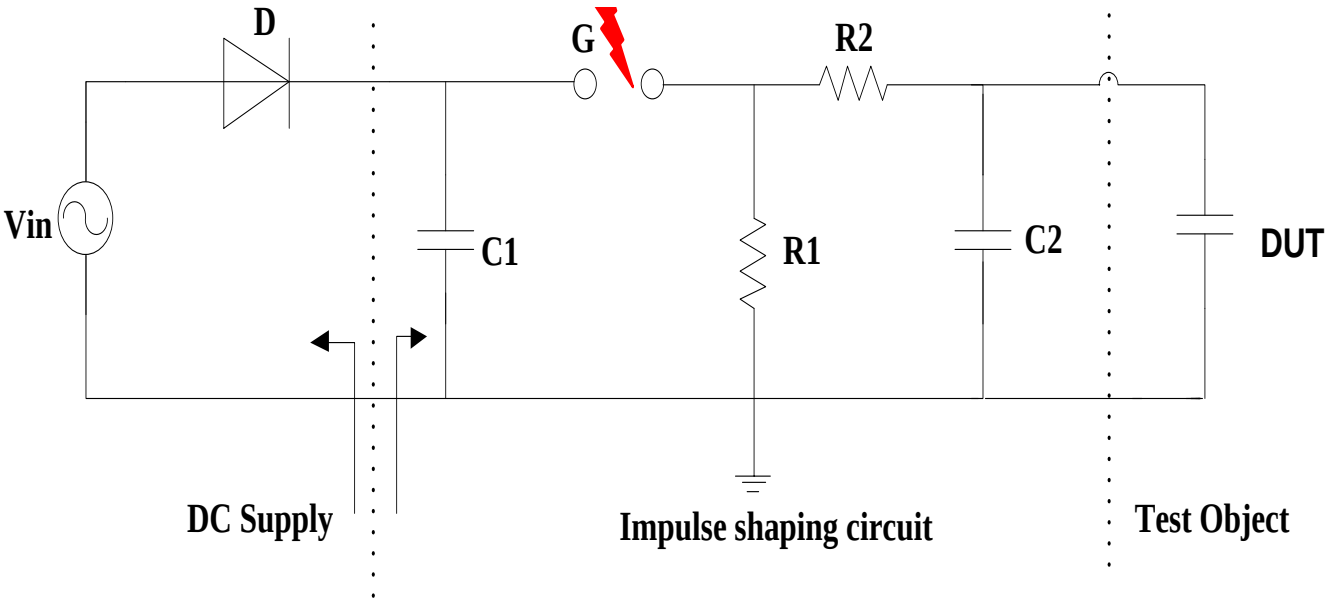

Vin – supply voltage

D – diode bank

C1 – charging capacitor

G – trigger gap

R1 – charging resistor

R2 – discharging resistor

C2 – discharging capacitor

DUT – test object

Figure 4-2: A single stage generator circuit

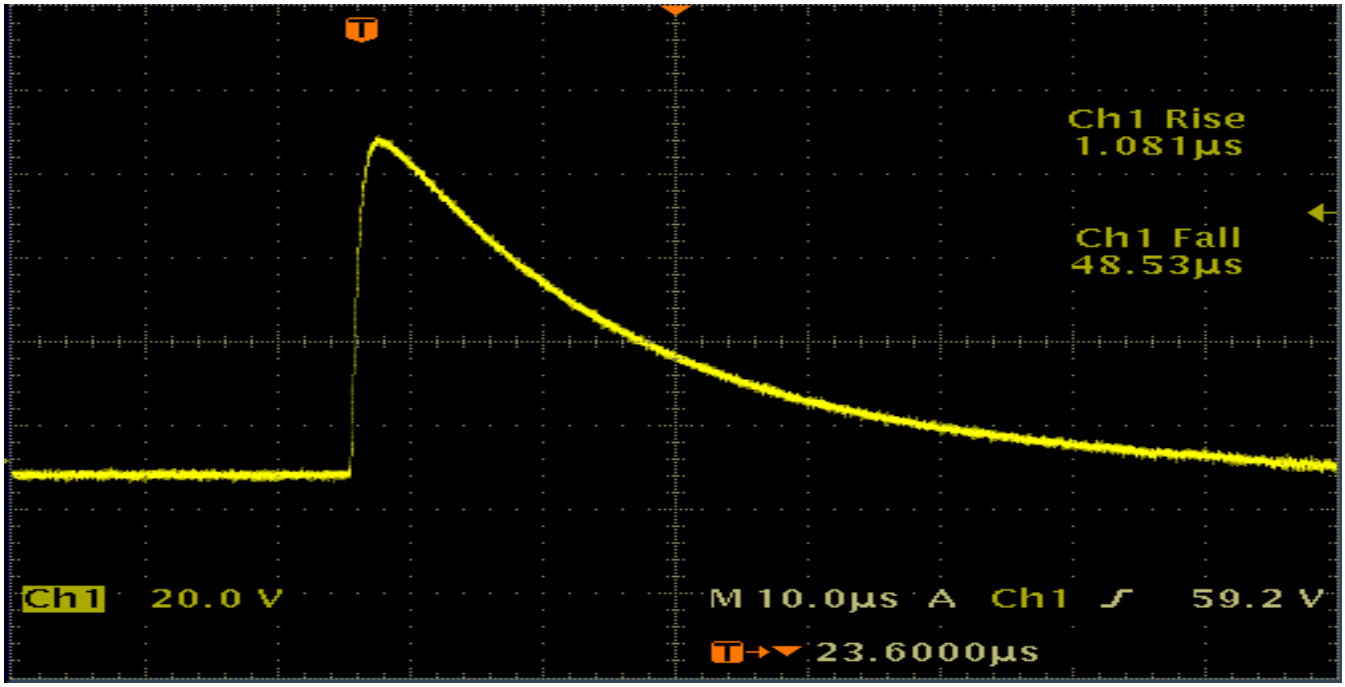

Figure 4-3: Output waveform of the impulse ageing test

Cavity defects were introduced in the power cable test samples after the impulse ageing experiment. The power cable test sample preparation process is described in the following section.

4.3 Test sample preparation

The preparation procedure entailed conditioning of power cable test samples for experimental tests. XLPE power cables were cut into 1 meter length segments. This length was deemed optimal to minimize signal attenuation and reflections that might be experienced with a longer cable (Grzybowski, 2007). The power cable segment ends were cast in epoxy resin in order to decrease the electric field concentration at both ends, and consequently prevent flashovers and surface discharges during impulse ageing and PD measurements respectively. A total of twelve power cable segments were prepared for testing and half of the samples were exposed to lightning impulses. Artificial cavity defects were created in the impulse-aged and un-aged test samples. A picture of one of the prepared power cable samples is illustrated in Figure 4-4.

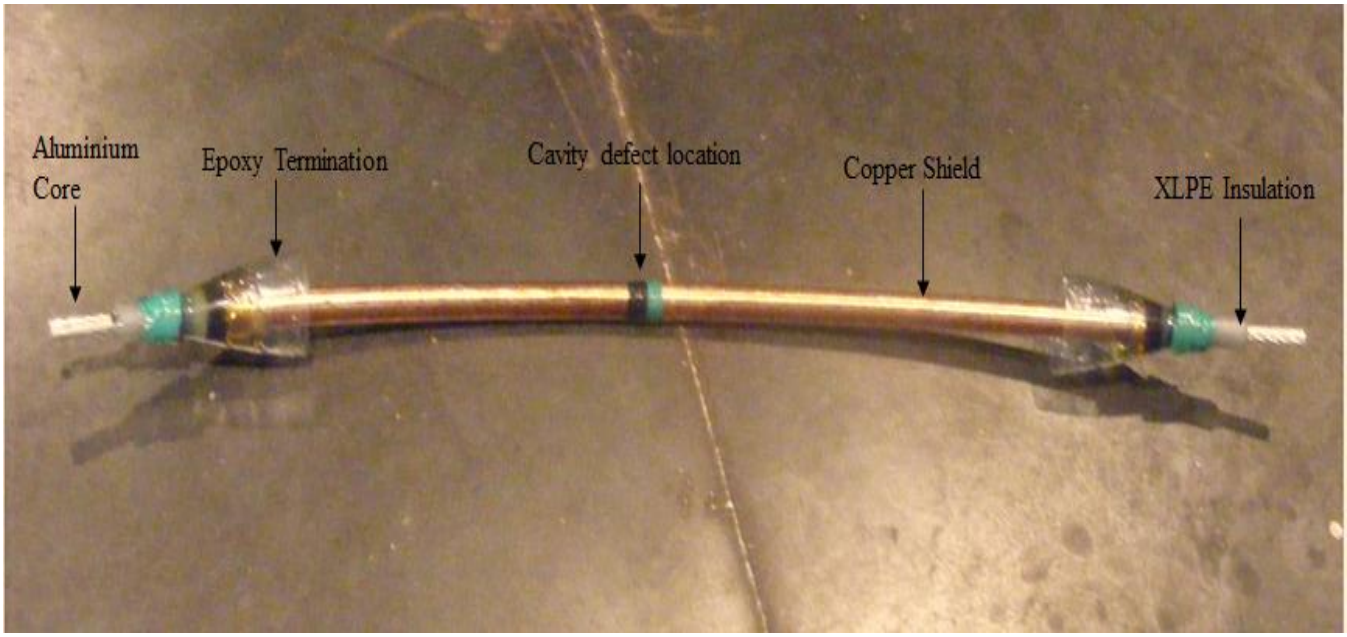

Figure 4-4: A power cable test sample

The creation of PD defects within the XLPE insulation was an elaborate process. The cavity defects were to be identical in geometric shape and dimensions. Prior to creating PD defects, a PD test was performed under normal operating conditions (6.35 kV phase voltage) on the terminated test samples to check if the samples were PD free. The PD test was performed according to the IEC 60270 standard PD

testing method. These power cable test samples with unintentional manufacturing PD sources were discarded and replaced with PD free test samples. PD defects were created only in PD free test samples. It was essential to ensure that there were no existing PD sources within the power cable test samples and that future PD behaviour was a result of the purposely introduced PD defects.

A cross-sectional view of the power cable test samples is illustrated in Figure 4-5. The Aluminium core carries the load current. The inner semiconducting layer prevents stress enhancement along interface between insulation and metallic core. The XLPE insulation provides electrical and mechanical separation between the cable core and the rest of the components. Outer semiconducting layer prevents stress enhancement along interface between insulation and outer metallic shield. The PVC sheath protects the cable from environmental elements.

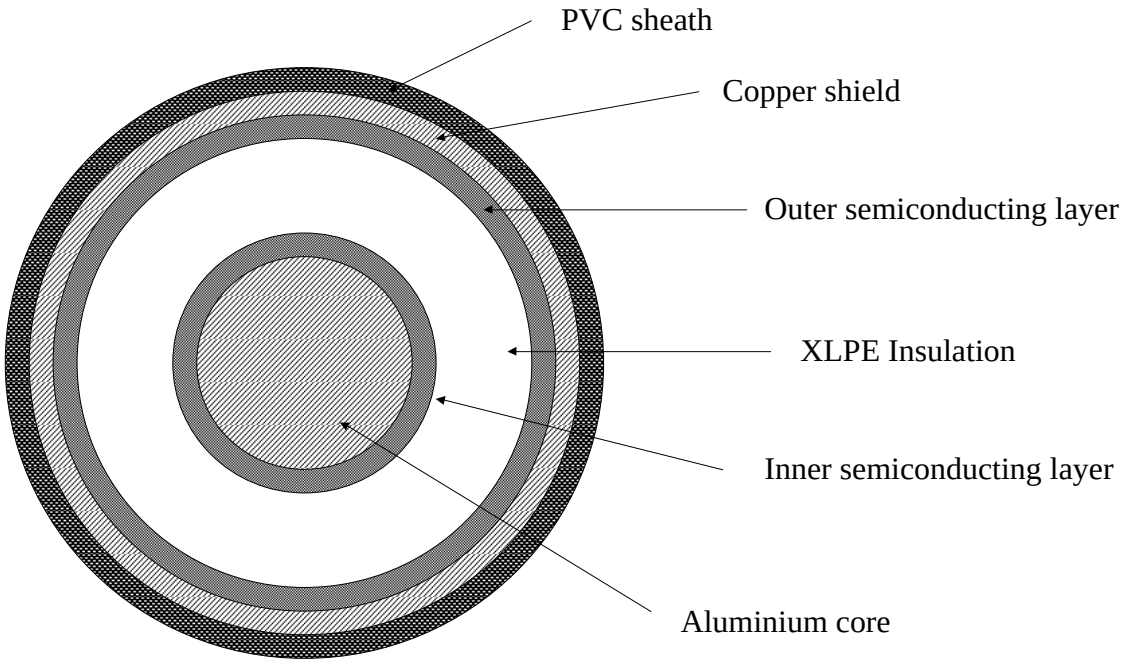

Figure 4-5: A cross-sectional view of a power cable test sample

A schematic of a cylindrical cavity defect is illustrated in Figure 4-6 where a and b are the cavity defect radius and height, respectively. Cavity defect dimensions play an essential role in influencing PD behaviour thus the required cavity defect dimensions had to be purposely determined. The aim of

choosing specific cavity dimensions was to ensure that most of the cavity defect area would be optimally exposed to PD activity. This is called the effective discharge area (Nyamupangedengu, 2011).

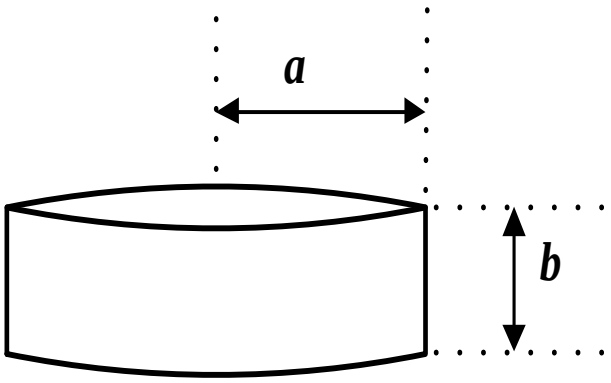

Figure 4-6: A disc void with radius a and height b

The cavity defect radius was calculated using the notion of effective discharge area and is expressed analytically as in Equation 4.1 (Wetzer, Pemen, & van der Laan, 1991):

$$a_{eff} = A\left\{1 - e^{-a/A}\right\} \tag{4.1}$$

Where:

a_{eff} = effective void radius [m]

a = actual void radius [m]

A = 2.147

Figure 4-7 is a plot of the effective radius as a function of the actual cavity radius. It indicates that defect cavity volumes with small radii avail optimum space to PD activity (Nyamupangedengu & Jandrell, 2007). Large cavity radii could render most of the cavity area redundant for optimum PD activity. Using Figure 4-7 an actual cavity radius of 1.5mm was chosen as it yields a negligible redundant space. Furthermore there is also a restriction on cavity height as well. It should be sufficiently small to avoid overstressing the remaining part of the adjacent insulation. This may be detrimental and cause the power cable to fail due to an intense field concentration. The thickness of the XLPE insulation on the 11 kV power cables is 3 mm, thus the cavity height was chosen to be a third of the XLPE power cable insulation thickness that is 1 mm. (Nyamupangedengu, 2011). A cylindrical, 3 mm diameter and 1 mm depth cavity defect was created within the XLPE insulation in both sample sets and covered with the copper shield.

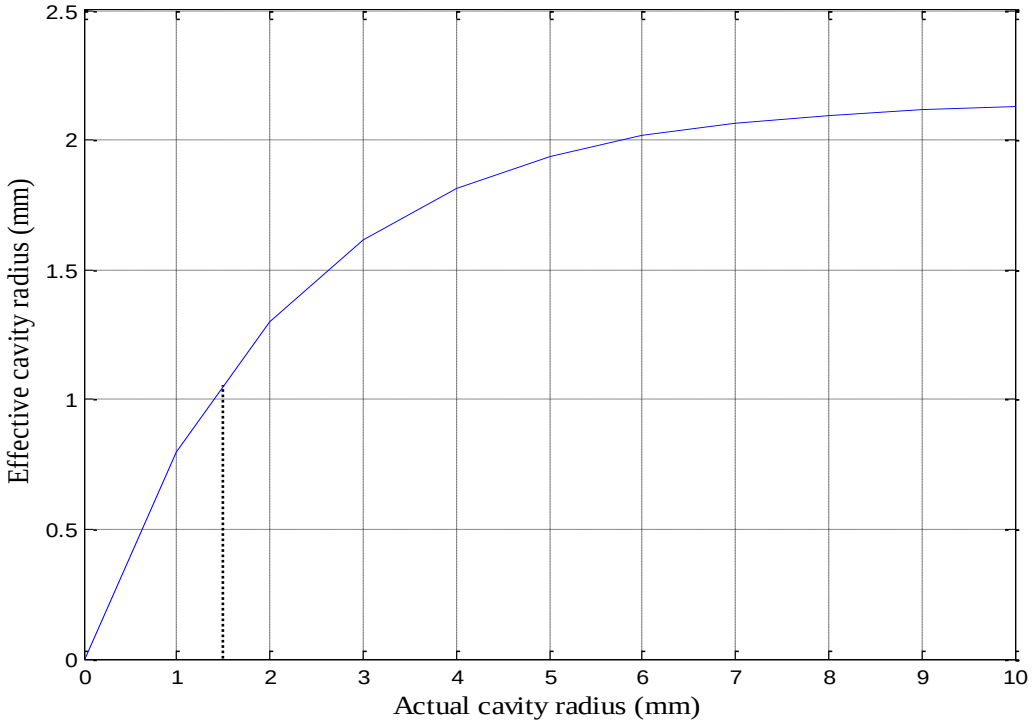

Figure 4-7: A plot of the effective radius (a_{eff}) of cavity exposed to PDs as a function of the actual cavity radius (a). (Nyamupangedengu & Jandrell, 2007)

A cross sectional view of the power cable test sample with an embedded artificial cavity is illustrated in Figure 4-8.

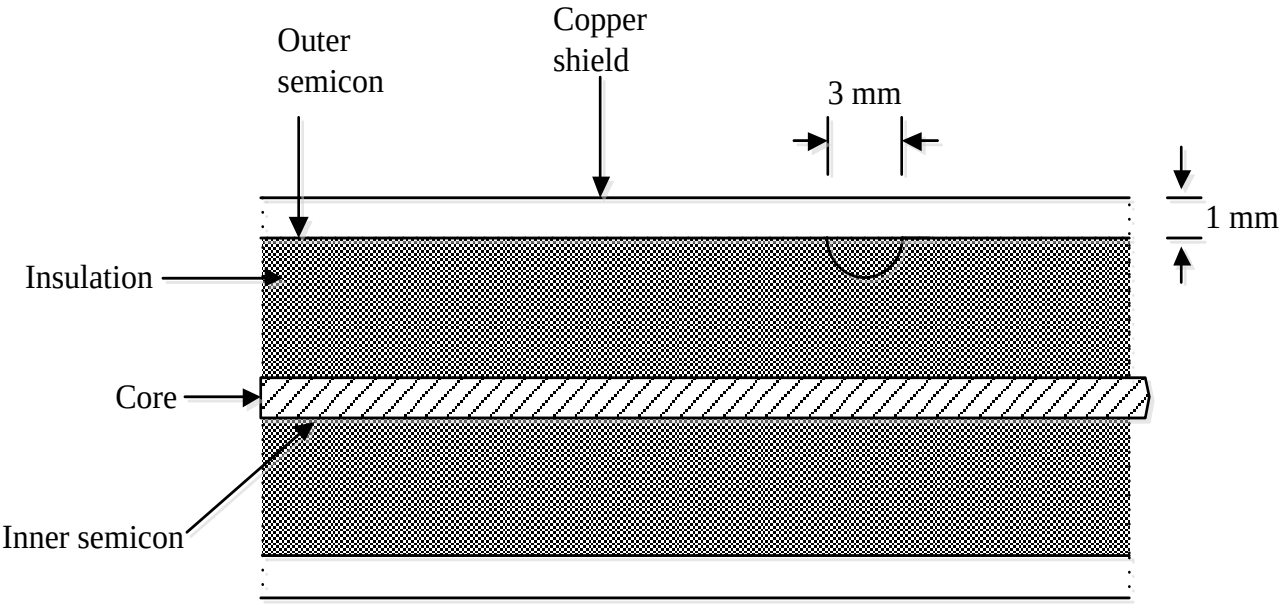

Figure 4-8: A cross sectional view of the cable sample with an artificial cavity

4.4 Partial discharge test setup

Partial discharge measurements were performed on all power cable test samples to verify that only PD free samples were used in the subsequent experiments. After the impulse ageing experiment and creation of artificial defects within the test samples, PD measurements were performed on all the samples.

Prior to PD testing it was necessary to calibrate the PD test circuit to ensure that the measuring system was able to measure the PD characteristics accurately. Figure 4-9 illustrates the IEC 60270 PD testing circuit diagram used to test for PDs in the un-aged and impulse-aged power cable samples respectively. One power cable test sample at a time was connected to the PD detection circuit. In order to calibrate the PD test circuit, a charge pulse was injected into the circuit at the high voltage connection of the test samples. The calibration process was performed with the PD test circuit un-energized to protect the calibration instrument from electrical shock. The calibration process involved adjusting the ICM Compact PD instrument settings such as signal gain and calibration charge.

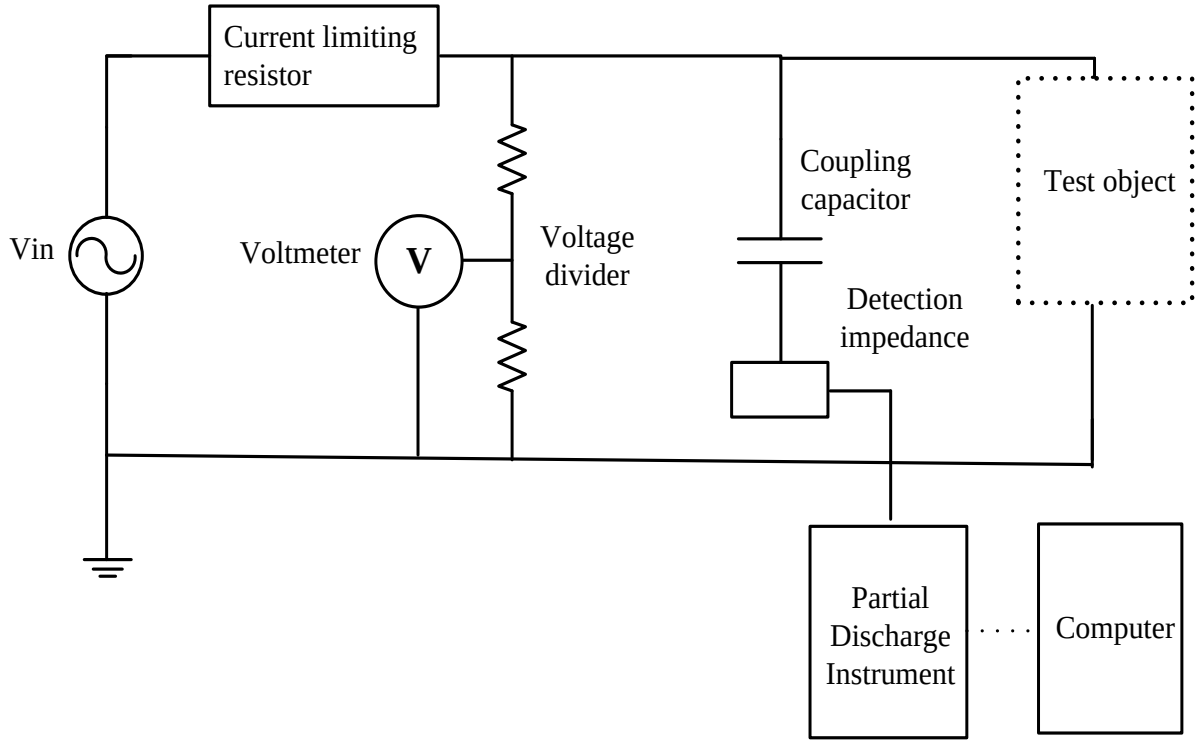

Figure 4-9: The IEC 60270 partial discharge test setup

The PD test circuit operates as follows: V_{in} supplies AC voltage to the PD test circuit. The current limiting resistor provides protection to circuit components and the source under fault conditions. The coupling capacitor replenishes the charge lost in the power cable test samples during a PD event. This "lost charge" causes a PD current to flow through the detection impedance and is detected by the PD measuring instrument. The former is connected to a computer for measurement display and records. After the PD test circuit was calibrated, noise levels were recorded at 6.35 kV (phase voltage) to distinguish between ambient noise and PD signals. Figure 4-10 is a snapshot of ambient noise at the phase-voltage. The ambience noise was sufficiently low <1 pC and consequently allowed for sensitive and accurate PD measurements.

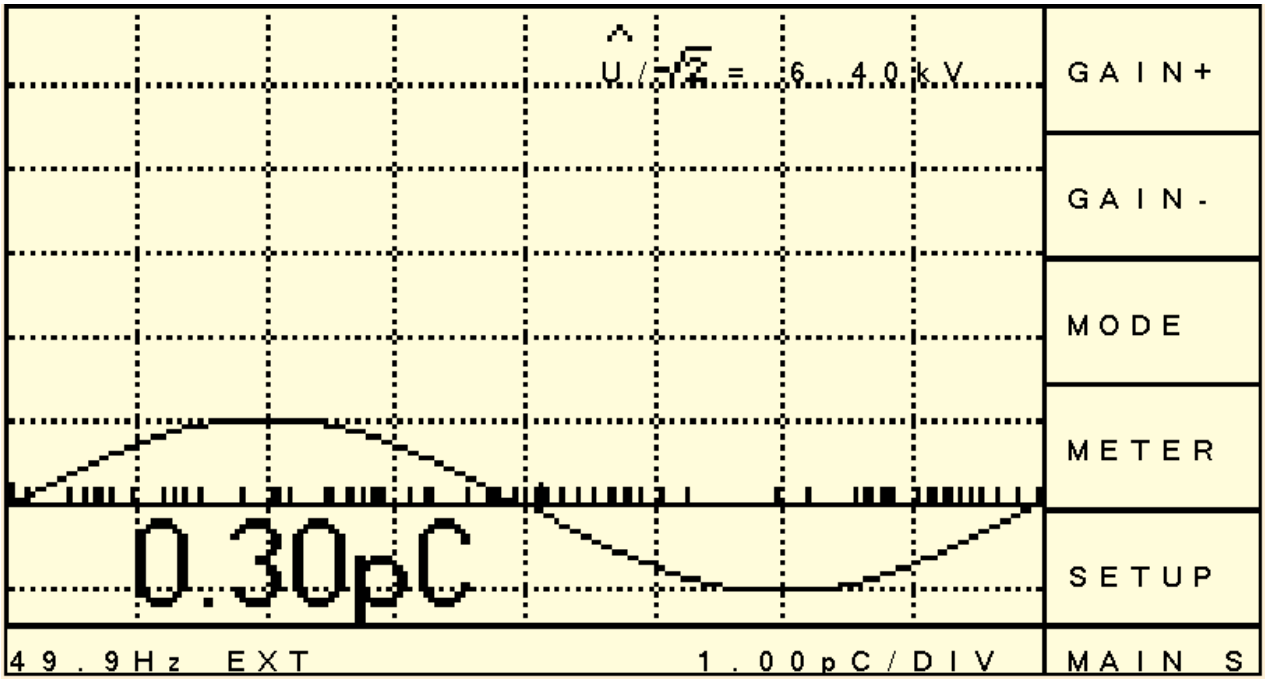

Figure 4-10: A snapshot of ambient noise measured at 6.35 kV

4.5 Conclusions and pointers to the next chapter

The tasks and experimental system developments performed prior to testing have been presented. These are the power cable test sample preparation, impulse generator circuit design and PD test measurement setup. The principles of operation of the single stage impulse generator circuit and PD detection test circuits were presented. The next chapter presents the experimental work performed in this research namely; pre-aging PD test, impulse ageing experiment and post-aging PD test experiment.

5 THE EXPERIMENTAL TESTS

The experimental work comprised of three main stages, namely; pre-aging PD measurements, impulse ageing and post aging PD measurements. These experiments were conducted on two sets of new 11 kV, 1 meter, XLPE cable segments. Each sample set consisted of six XLPE power cable segments. The aim of the pre-aging PD experiment was to confirm that the test samples were PD free. The aim of the impulse ageing experiment was to age the test samples with standard lightning impulses. The purpose of the post-aging PD measurement was to compare cavity PD characteristics in impulse aged and un-aged insulation. PD characteristics of interest were PD magnitude, PDIV (partial discharge inception voltage) and PDPRP (partial discharge phase resolve patterns) as they characterize the PD process.

5.1 Pre-ageing PD test

The pre-aging PD test was performed according to the IEC 60270 standard PD testing method. The pre-aging PD test was performed at 6.35 kV which is equivalent to the rated phase operating voltage of an 11 kV power cable. The voltage was applied for 4 hours before declaring the cable PD free.

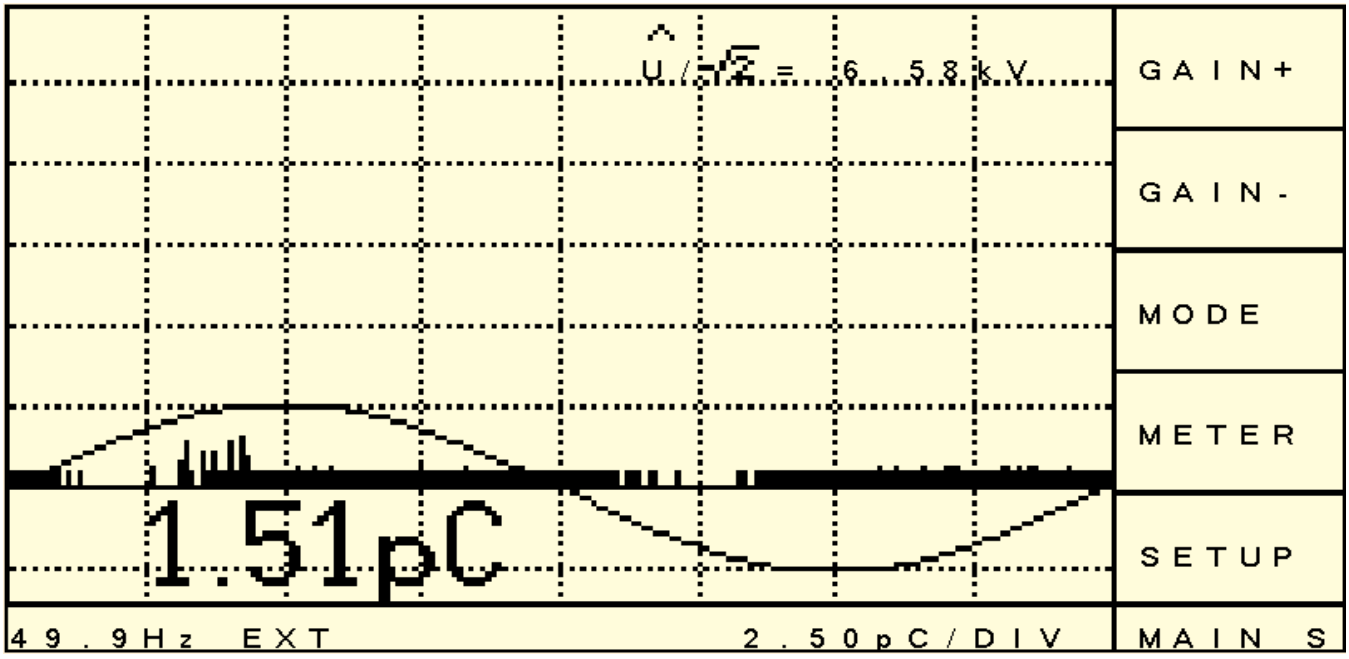

Figure 5-1: An example of a phase resolved patterns of a power cable sample without PD activity at operating voltage

Figure 5-1 shows an example of a phase resolved pattern of a PD free power cable sample operating at the phase voltage. Power cable samples that displayed PD activity were rejected and only cables that are PD free were used in the subsequent experiment.

5.2 Impulse ageing procedure

In this experiment, lightning impulses are used to electrically age new power cable test samples. A set of six PD free, power cable test samples was subjected to 5000, 40 kV_{rms}, 1.2/50 µs lightning impulses. The power cable samples were aged with 5000 lightning impulses as these were deemed sufficient for optimum ageing of the power cable samples and this was based on similar work by (Dao, Lewin, & Swingler, 2009) and (Grzybowski, 2007). The peak value of 40 kV was chosen based on the insulation level of the XLPE test samples. Insulation level is defined by the magnitude of test voltages which the equipment insulation under test should be able to withstand. In this research the XLPE insulation value of 11 kV (peak) corresponds to a standard lightning impulse withstand voltage of 40 kV peak (Kuffel, Zaengl, & Kuffel, 2000).

The schematic and actual picture of the impulse ageing setup are depicted in Figure 5-2 and Figure 5-3 respectively. The power test samples were connected in parallel and stressed simultaneously as shown in Figure 5-3. The AC supply voltage was raised gradually until it yielded 40 kV dc on the dc bus bar. At 40 kV dc, gap G is triggered. Capacitor C1 and capacitor C2 are charged through resistor R1 and discharged through resistor R2. The values of R1 and R2 were selected using an iteration method. The DUT (power cable samples) are subjected to the transient lightning impulses through capacitor C2. The repetition rate of applying the lightning impulse was one impulse every 30 seconds. The output waveform has a rise time of 1.08 µs and a fall time of 48.53 µs. The output waveform of the lightning impulse generator had a tolerance band of 1.2/50 µs ± 5%. This was acceptable as it was within limits deemed standard for lightning impulses 1.2/50 µs ± 30/20% (Kuffel, Zaengl, & Kuffel, 2000). The impulse ageing experiment was completed in four weeks. After this, cavity defects were created in both un-aged and impulse-aged test samples for comparative PD measurements as presented in the next section.

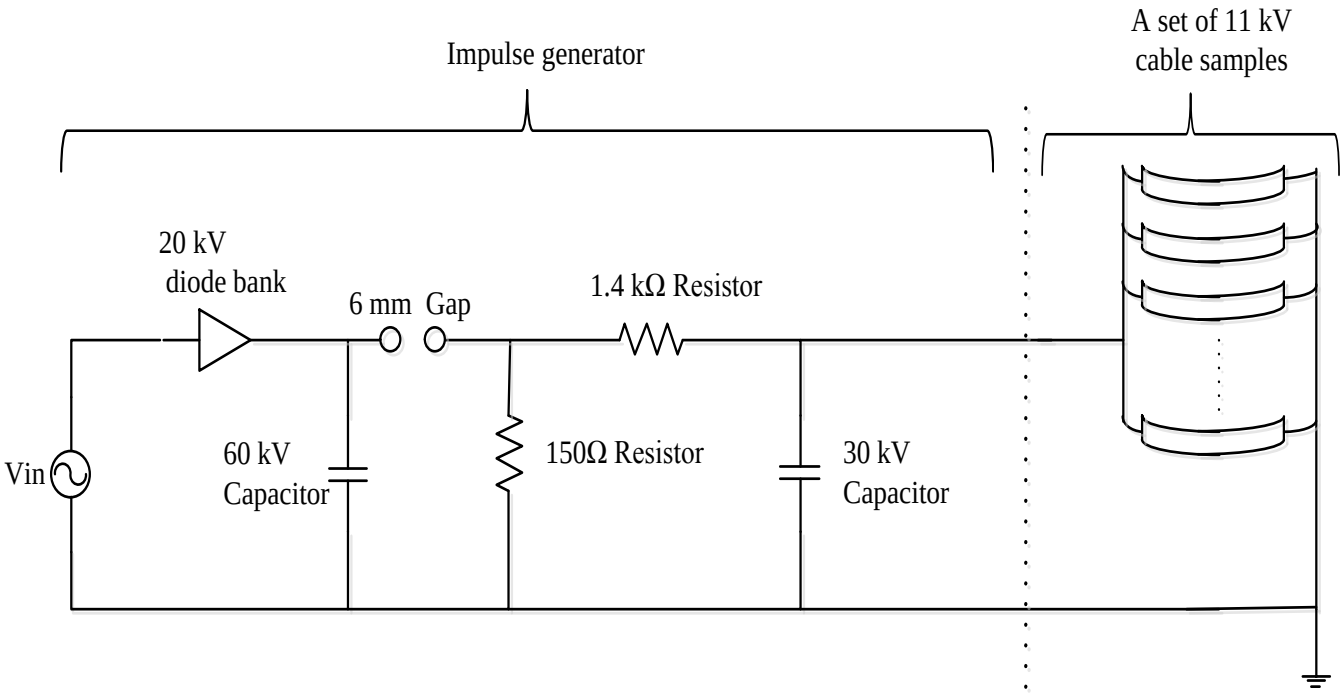

Figure 5-2: A schematic of the impulse ageing circuit

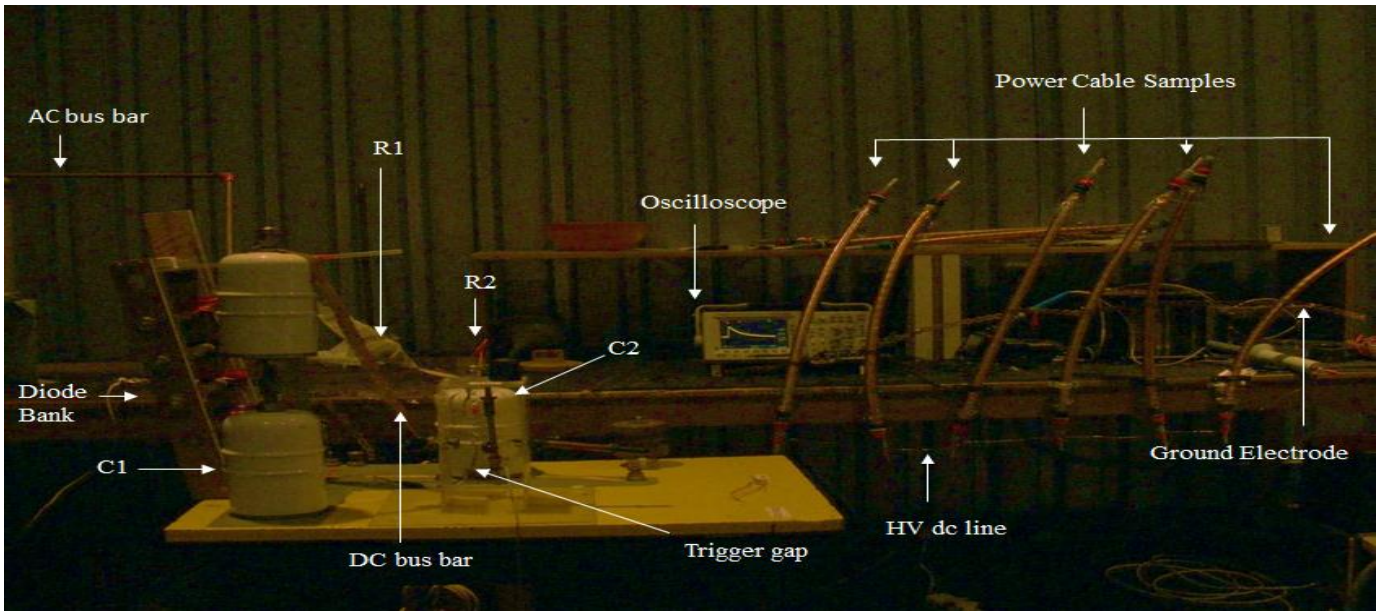

Figure 5-3: A picture of the impulse ageing test setup

5.3 Post-ageing PD test

The PD characteristics of interest in this research were PDIV, PD magnitude and PDPRP. Prior to recording the PD signals, the samples were preconditioned by energizing the samples at 9.4 kV (1.5 times the cable phase voltage) for a duration of 2 hrs. This is common practice to achieve steady PD behaviour (Nyamupangedengu & Jandrell, 2007). Precautions were taken to keep the insulation surface of the power cable samples clean and dry because humidity or pollution on insulating surfaces could affect PD behaviour. The PD measurements were generally taken at 25 ºC and 830 – 850 mbar Johannesburg atmospheric pressure at an altitude of 1750 m. A rest interval of 2 hours after impulse ageing tests was necessary to ensure good reproducibility of PD tests (SABS-IEC60270, 2001).

5.3.1 PD inception voltage measurement procedure

One power cable test sample at a time was connected to the PD test circuit and the samples were tested consecutively. The PD inception measurements were performed according to IEC60270 PD testing method. The supply voltage was raised gradually until PDs were detected in the test sample. The PD inception voltage was recorded at this instance. Ten PDIV measurements were taken for each power cable test sample.

5.3.2 PD magnitude measurement procedure

It was necessary to select a constant test voltage level for PD magnitude measurements other than PD inception voltage in order to acquire reproducible results. This was a result of different measured PD inception voltage in both the un- aged and impulse-aged power cable test samples. Therefore, PD magnitude was measured at a voltage level of 12 kV it was slightly higher than the average measured PD inception voltage of un-aged and impulse-aged test and thus provided steady PD activity. Ten PD magnitude measurements were recorded over duration of 30 seconds for each power cable sample using a continuous PD data logging function on the ICM compact PD measurement instrument. Ten measurements were recorded for each sample to take into account the statistical variations of the PD process. Figure 5-4 and Figure 5-5 show the schematic of the PD measurement setup and actual picture respectively.

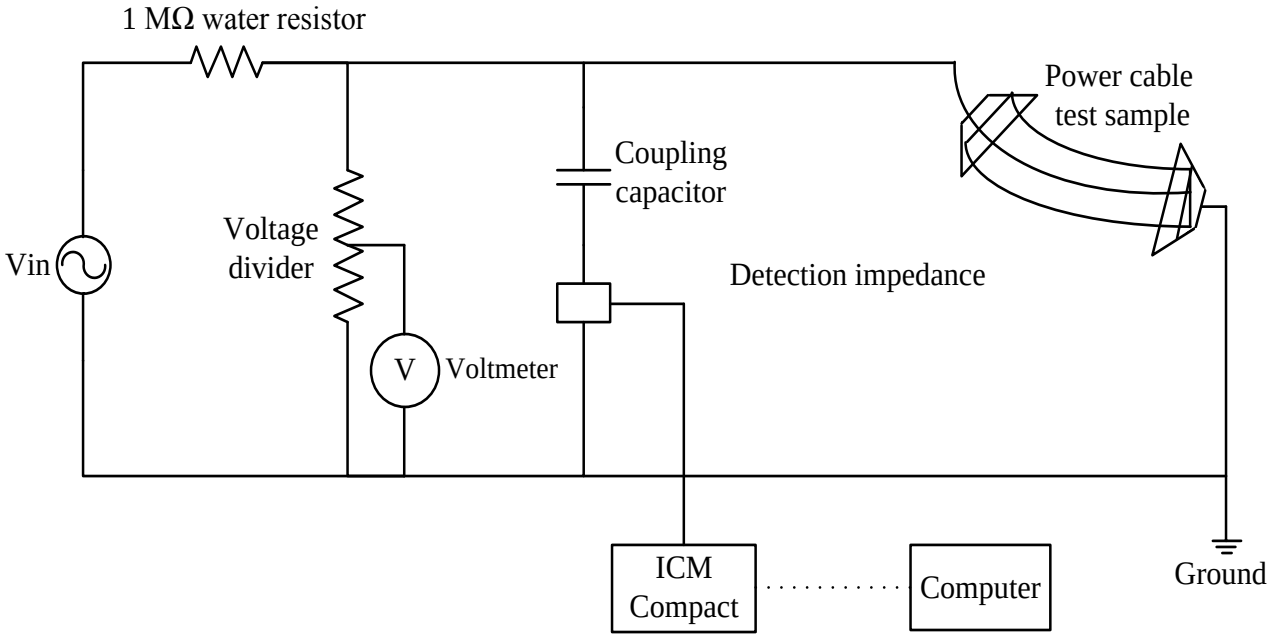

Figure 5-4: A schematic of the partial discharge test setup

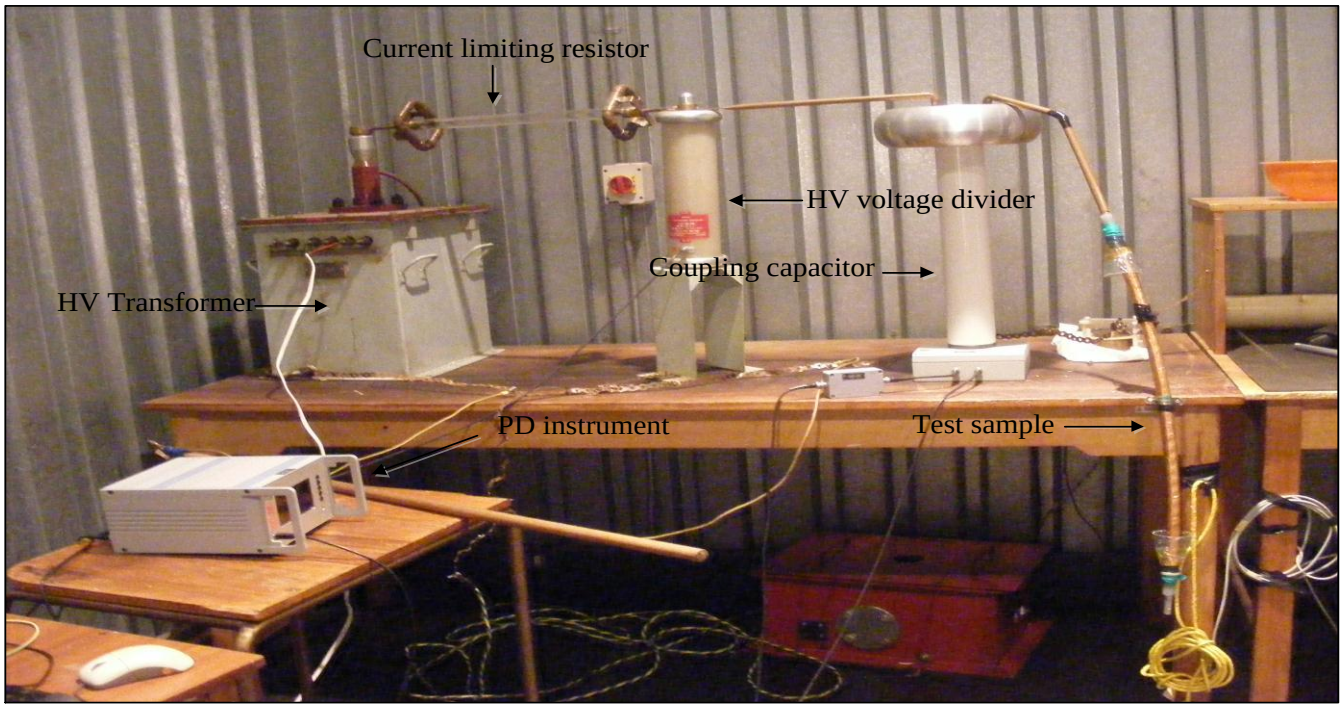

Figure 5-5: A picture of the IEC 60270 PD test setup

5.3.3 PD phase resolved pattern measurements procedure

PD phase resolved patterns were also recorded at 12 kV similar to PD magnitude measurements. PD phase resolved patterns are also a function of the supply voltage, as such 12 kV was a chosen voltage level for all the PDPRP measurements. PDPRP were captured over duration of five minutes for each sample on the ICM compact PD measuring instrument in the hold mode. Five minutes was adequate to capture a clear PDPRP shape that did not clutter the PD instrument measurement screen. The magnitude, duration and pulse repetition rate of PD pulses can be significantly affected by the time of voltage application as PD behaviour evolves over time (Morshuis & Kreuger, 1990). Also, the measurement of different quantities related to PD pulses usually presents larger uncertainties than other measurements during high-voltage tests. Figure 5-6 gives a picture of the ICM Compact PD measuring instrument.

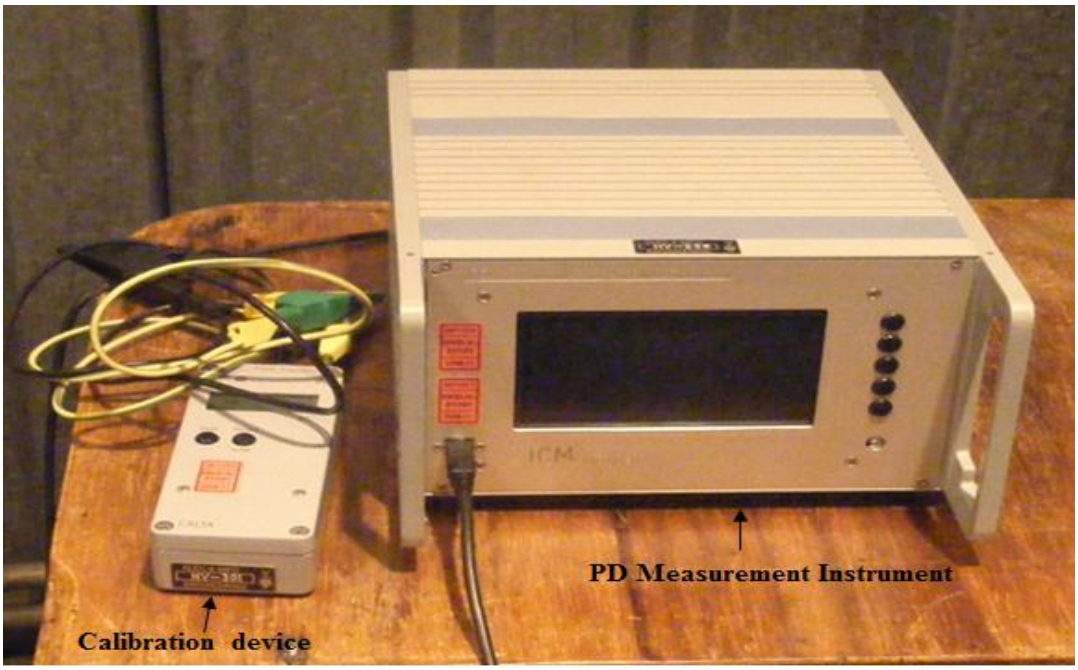

Figure 5-6: A picture of the ICM Compact PD measuring instrument

5.4 Conclusions and pointers to the next chapter

The experimental work conducted in this research has been presented in the following order: pre-aging PD test, impulse ageing test and post-aging PD test. The experimental procedures altogether with the corresponding standards of these experiments have been presented. The next chapter presents the

experimental measurement results and discusses the measured PD characteristics of un-aged and aged test samples.

6 THE EXPERIMENTAL MEASUREMENT RESULTS AND DISCUSSION

This chapter presents measurement results of experiments on the behaviour of PDs in impulse aged insulation. This was achieved by measuring the following PD parameters: PD phase-resolved patterns, PD magnitude and PD inception voltage. The findings of the PD characteristic measurement results are then analysed and discussed.

6.1 PD Phase resolved patterns measurement results and analysis

PD phase resolved patterns were captured using the PD Diagnostix ICM Compact® PD measuring instrument in the hold mode. The purpose of PDPRP measurements was to study the effect of impulse ageing of insulation on PDPRP. This was achieved by recording PDPRP patterns in un-aged and impulse-aged power cable test samples and comparing the results. PDPRP parameters of interest were phase angle and peak PD magnitude profiles. PDPRP phase angle indicates the repetition rate of PD pulses and peak PD magnitude profiles are commonly used in practice to classify PD defects (Paoletti & Golubev, 2001).

The following sub-sections present and analyse PD phase resolved patterns of un-aged and impulse-aged power cable test samples and conclude with a discussion on the effect of impulse ageing on PD phase resolved patterns.

6.1.1 Un-aged power cable samples PD phase resolved patterns

Figure 6-1 to Figure 6-5 are PD phase resolved patterns recorded in un-aged power cable test samples. The following observations were deduced from the PDPRP diagrams as follows:

- Generally the maximum peak magnitude of the PDPRP positive half cycle is lower than that of the negative half cycle in the un-aged power cable test samples. However sample 5 was an exception it exhibited the opposite trait.
- The PD pulse profile of the positive half cycle tends to converge at the edges with mild skewness.

PD phase resolved patterns recorded in impulse- aged power cable test samples are presented in the subsequent sub-section.

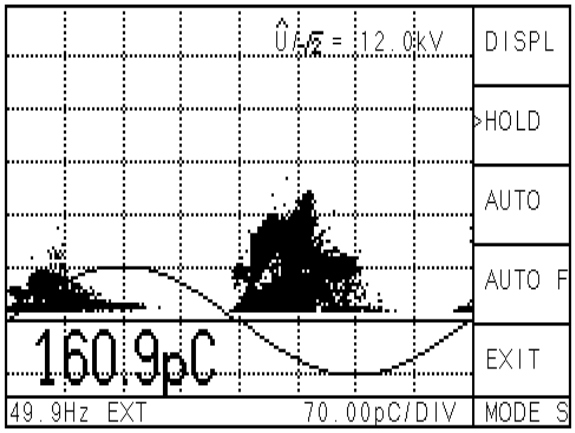

Figure 6-1: PDPRP of un-aged power cable sample 1

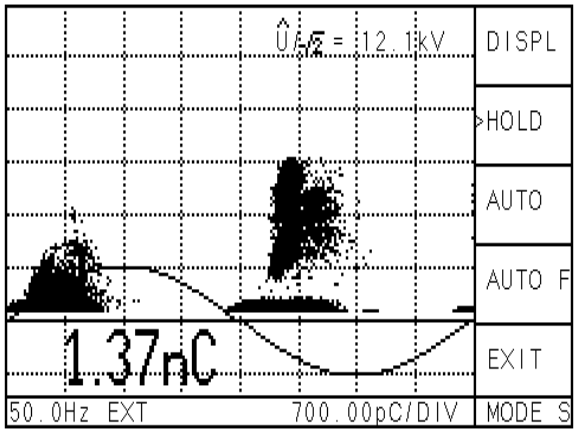

Figure 6-2: PDPRP of un-aged power cable sample 2

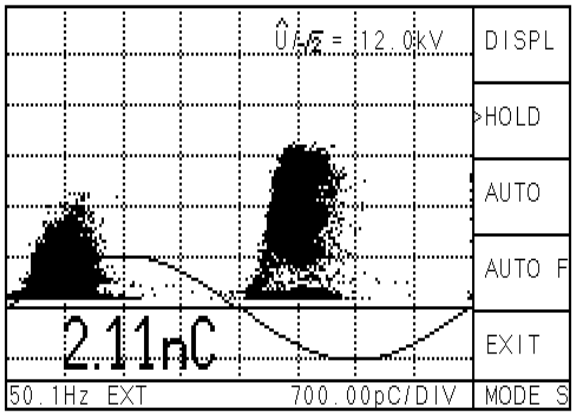

Figure 6-3: PDPRP of un-aged power cable sample 3

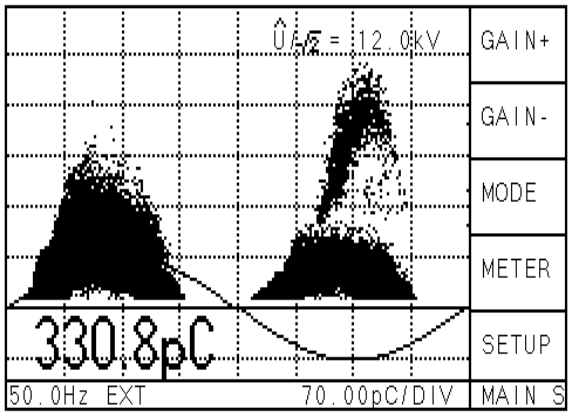

Figure 6-4: PDPRP of un-aged power cable sample 4

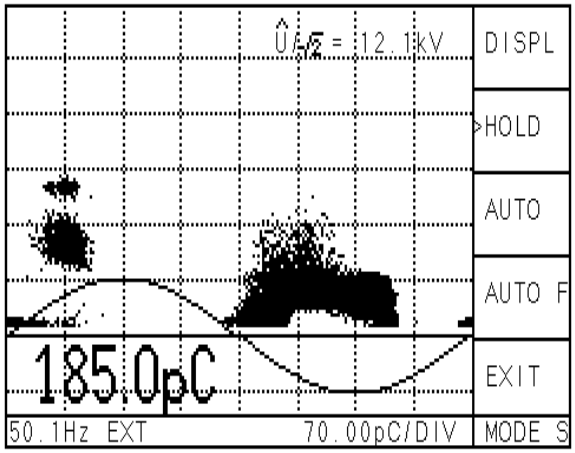

Figure 6-5: PDPRP of un-aged power cable sample 5

6.1.2 Aged power cable samples PD phase resolved patterns

The following figures are PDPRPs recorded in impulse-aged power cable samples:

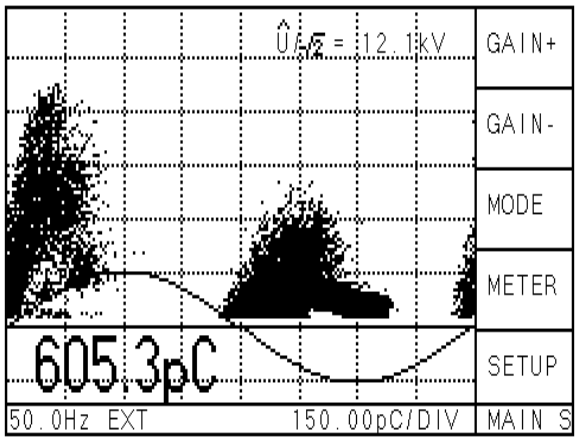

Figure 6-6: PDPRP of impulse aged power cable sample 1

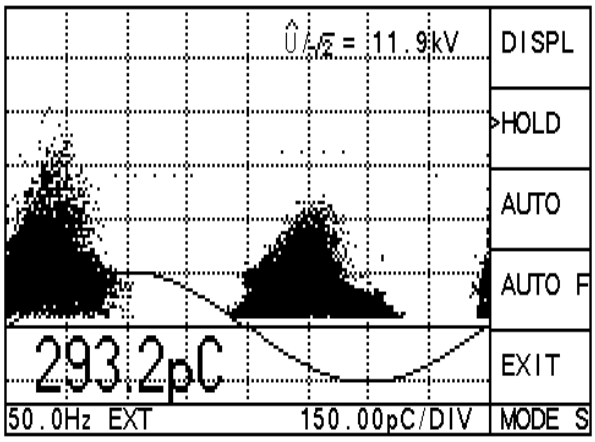

Figure 6-7: PDPRP of impulse aged power cable sample 2

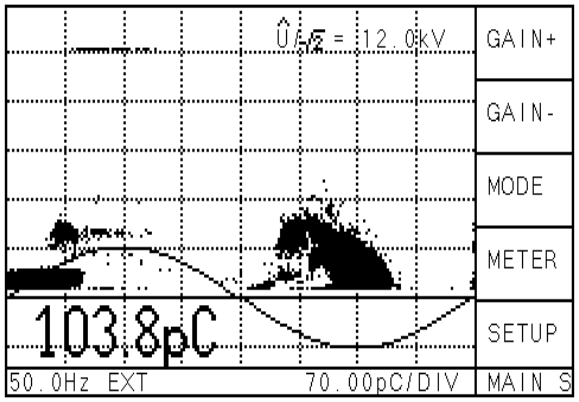

Figure 6-8: PDPRP of impulse aged power cable sample 3

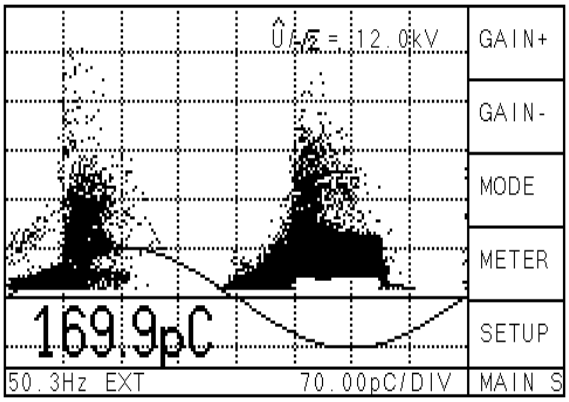

Figure 6-9: PDPRP of impulse aged power cable sample 4

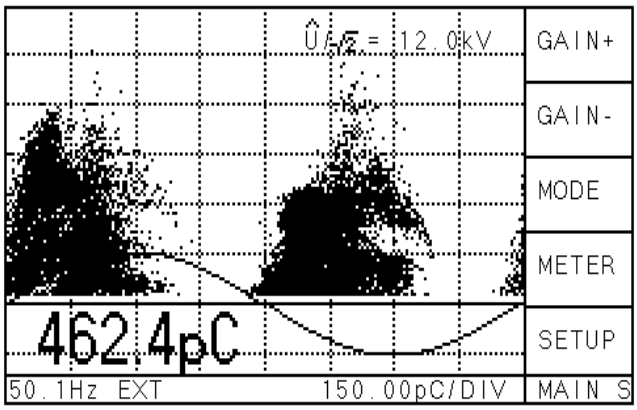

Figure 6-10: PDPRP of impulse aged power cable sample 5

A distinctive feature of PDPRP of impulse-aged samples is that the positive half cycle peak magnitude is higher than or equal to that of the negative half cycle. This is contrary to peak magnitude profiles in un-aged sample. These noteworthy observations are analysed and discussed in the following sub-section.

6.1.3 Analysis and discussion of PD phase resolved patterns results

A comparison of the ratios of positive half cycle peak magnitude to negative half cycle peak magnitude of un-aged and impulse-aged power cable test samples is depicted in Figure 6-11. Generally, PD phase resolved patterns magnitude peaks were higher in the un-aged power cable samples than in the impulse-aged power cable test samples. This was expected due to scarce PD initial electrons in the un-aged cavity environment. PD pulses were distributed over a wider phase angle in the impulse-aged power cable test samples than in the un-aged test samples. This indicates a rapid PD repetition rate and implies that there was an abundance of PD initiating electrons in the impulse-aged cavity. This was expected as lightning impulses in insulation may generate excited electrons with high energy that penetrate the bulk dielectric (Mason, Wilson, Given, & Fouracre, April 2008).

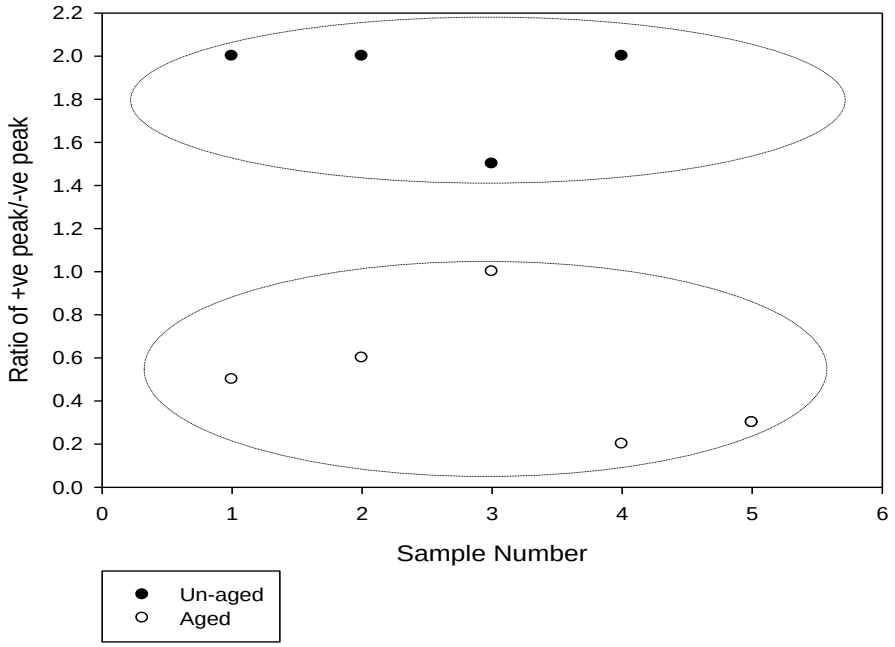

Figure 6-11: Comparison of negative PD magnitude between un-aged and aged sample set

In the event of PD activity within an enclosed cavity between XLPE insulation and copper as illustrated in Figure 6-12, the different materials play alternating anode and cathode roles in the positive and negative PD half cycles respectively (Paoletti & Golubev, 2001). The cathode material provides the electrons required to initiate and sustain the PD process. The conducting characteristics of copper are such that it is an electron deficient cathode in comparison to the XLPE insulation material. When the former takes on the cathode role, and PD activity occurs on the insulation layer, the non-conducting characteristics of the insulation create plasma. Plasma stimulates PD activity as it is a very good source of free electrons. Consequently, there is a higher probability of PD activity occurring when the insulation material is the cathode. Therefore, there is a relationship between PD phase resolved patterns peak magnitude profiles and role of the insulation material acting as the cathode or anode as shown in Figure 6-13. It is an example of a PDPRP measured in an un-aged power cable test sample.

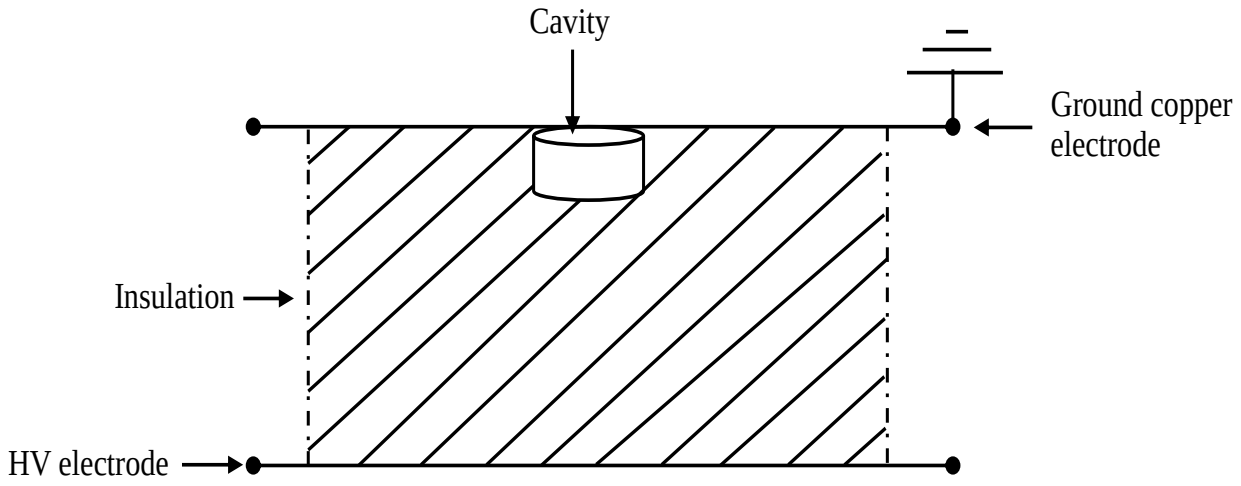

Figure 6-12: Insulation acting as the cathode at regions of greater electron flow

In the positive half cycle the copper material acts as the cathode and the insulation material acts as the anode. Electrons are released by the metal and are accelerated towards the insulation. The rate at which the electrons are released is governed by the work function of the metal (Kao & Demin, 2003). The work function of a material is the minimum energy necessary to remove an electron from a material. The copper material has a higher work function than XLPE insulation and consequently fewer electrons are released in the positive half cycle and this results in less PD activity as shown in Figure 6-13.

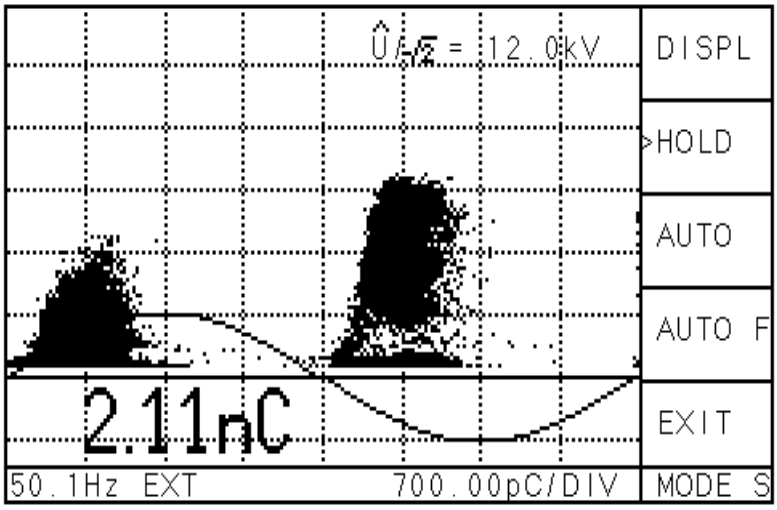

Figure 6-13: Positive half cycle and negative half cycle PD

In the negative half cycle the insulation material acts as the cathode and the copper material acts as the anode. Electrons are supplied by the insulation and there are abundant seed electrons in this case. Hence there is a higher occurrence of PD activity in the negative half cycle as displayed in Figure 6-13. This agrees with the measured PD phase resolved patterns of un-aged power cable test samples and explains the observed lower peak magnitude profiles in the PD phase resolved patterns of the impulse-aged cable samples.

When a lightning impulse is applied across a copper–insulator–copper configuration, electrons will be inserted into the insulation in three possible ways: (1) Schottky emission, (2) thermally assisted tunnelling, and (3) tunnelling by traps (Niemeyer, 1995), (Kao & Demin, 2003). Polymer insulation intrinsically comprises of a large quantity of microscopic traps. Impulse ageing of insulation injects electrons into these traps and this results in trapped space charges (Kao & Demin, 2003). As a result, PD initiating electrons inside the insulation and the plasma on the insulation layer are augmented. Furthermore the bombardment of the insulation surface with electrons during impulse ageing may reduce the work function of the insulation.

PD magnitude peaks of impulse-aged power cable test samples was lower than that of un-aged power cable test samples due to the reduced waiting period of PD initiating electrons. It is therefore suggested that the observed differences between PDPRP of impulse-aged and un-aged power cable test samples were attributed to changes in the insulation work function as a result of test samples' exposure to lightning. This area of research is fairly new and currently there is no literature available on the

influence of impulse ageing on PDPRPs; as such further work in this field is necessary. The next sub-section presents PD magnitude measurement results.

6.2 PD magnitude results and analysis

The following sub-sections contain PD magnitude measurement results and analysis. The effect of impulse ageing on PD magnitude is also discussed.

6.2.1 PD Magnitude results

This section contains plots of PD magnitude measurement results of un-aged and impulse-aged power samples. The charge magnitude of interest is the average charge (*Qp* Mean) as it contains the most information. However charge magnitude variants such as *Qp* Max and *Qp* Min are included in the appendix (section 8.1) in order to reveal additional information of PD magnitude data profile. Ten measurements of *Qp* Mean were taken for each test sample using an inbuilt function on the ICM Compact PD instrument over a 30 second period. These measurements are presented in Table 8-1 and Table 8-2 in the appendix, respectively. The PD magnitude data plots of un-aged and impulse-aged sample are depicted in Figure 6-14 and Figure 6-15 respectively. These show variations or repeatability of measurement results within the particular sample sets.

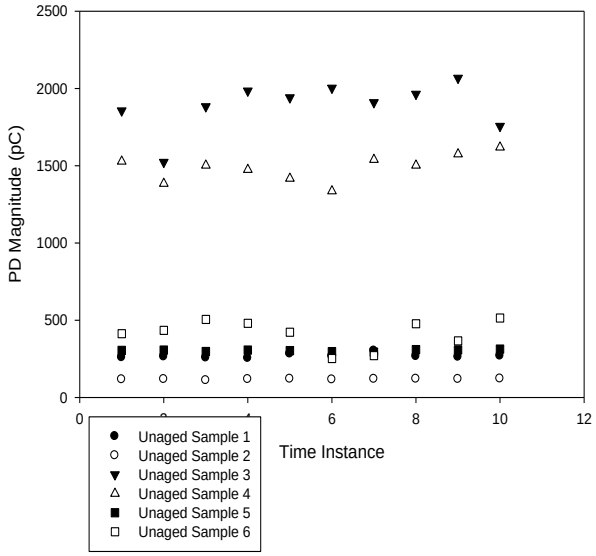

Figure 6-14: PD Magnitude within the un-aged sample set

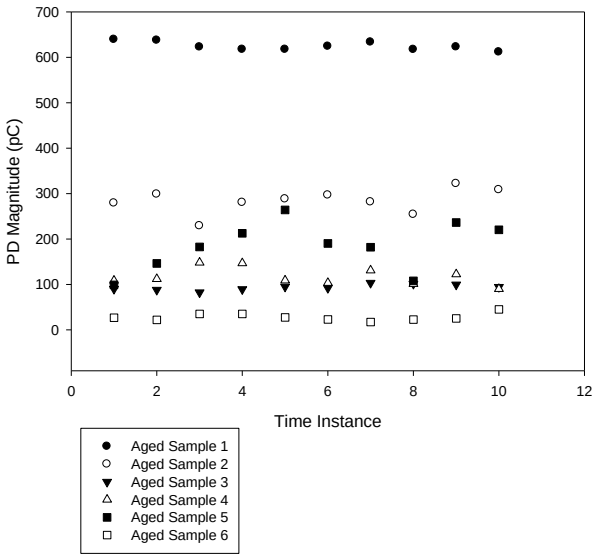

Figure 6-15: PD Magnitude within the impulse aged sample set

It was observed that mean PD magnitude values varied significantly within the sample sets, however *Qp* Mean data points of individual samples was minimal. In order to compare PD magnitude values between the un-aged and impulse-aged samples, an average of individual sample data points was calculated. The resultant was six PD magnitude data points of each sample set and a comparative plot of these points is given in Figure 6-16. Generally, PD magnitude of the un-aged power cable test samples was higher than that of impulse-aged test samples.

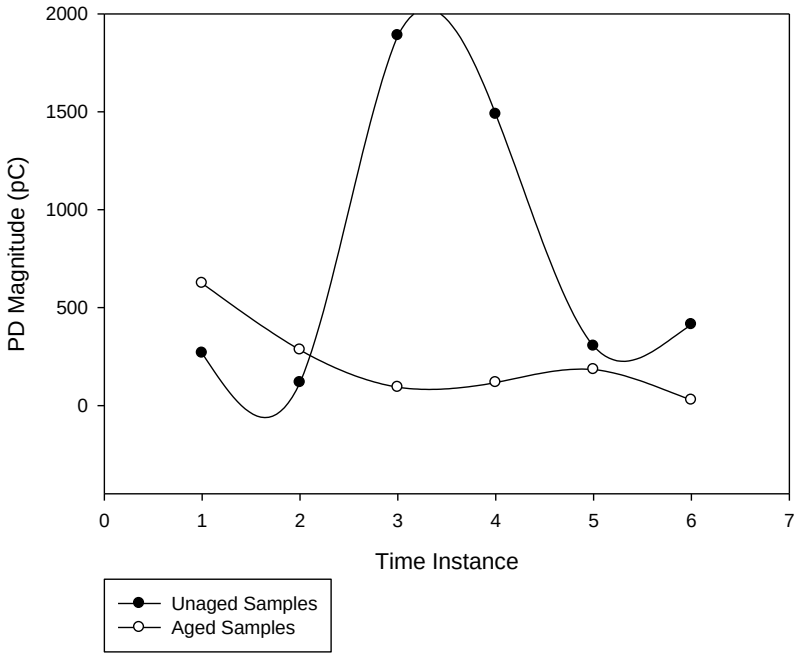

Figure 6-16: Comparisons of PD Magnitube between un-aged and impulse aged samples

Statistical variables of un-aged and aged power cable test samples were calculated in order to understand the statistical variation of PD magnitude data points. These are presented in Table 6-1.

Table 6-1: PD magnitude statistical variables of un-aged and impulse-aged power cable test samples

	Mean PD Magnitude		Standard Deviation	
	Arithmetic mean	% Difference	Standard deviation	% deviation
Un-aged	747 pC	70.28 %	692	71.09%
Impulse-aged	222 pC		200	

The PD magnitude data standard deviation (σ) of the un-aged power test samples is 692. It indicates that there is a large variance of un-aged PD magnitude data from the arithmetic mean. The corresponding arithmetic mean Á is 747 pC. The standard deviation (σ) of impulse-aged PD magnitude data is 200 pC. This is moderate in comparison to the standard deviation (σ) of un-aged PD magnitude data. The corresponding impulse-aged arithmetic mean Á is 222 pC.

Comparing the PD magnitude standard deviation and arithmetic mean between un-aged and impulse-aged power cable test sample sets reveals a significant magnitude difference of these values. This is supported by Figure 6-14, Figure 6-15 and Figure 6-16. The average PD magnitude (747 pC) of un-aged power cable test samples is significantly higher than that of the aged power cable samples 222 pC. PD magnitude measurements of impulse-aged insulation have a lower standard deviation than that of un-aged power cable test samples. The PD magnitude data points of the former exhibited a wide distribution as illustrated Figure 6-17 and this typifies a random process.

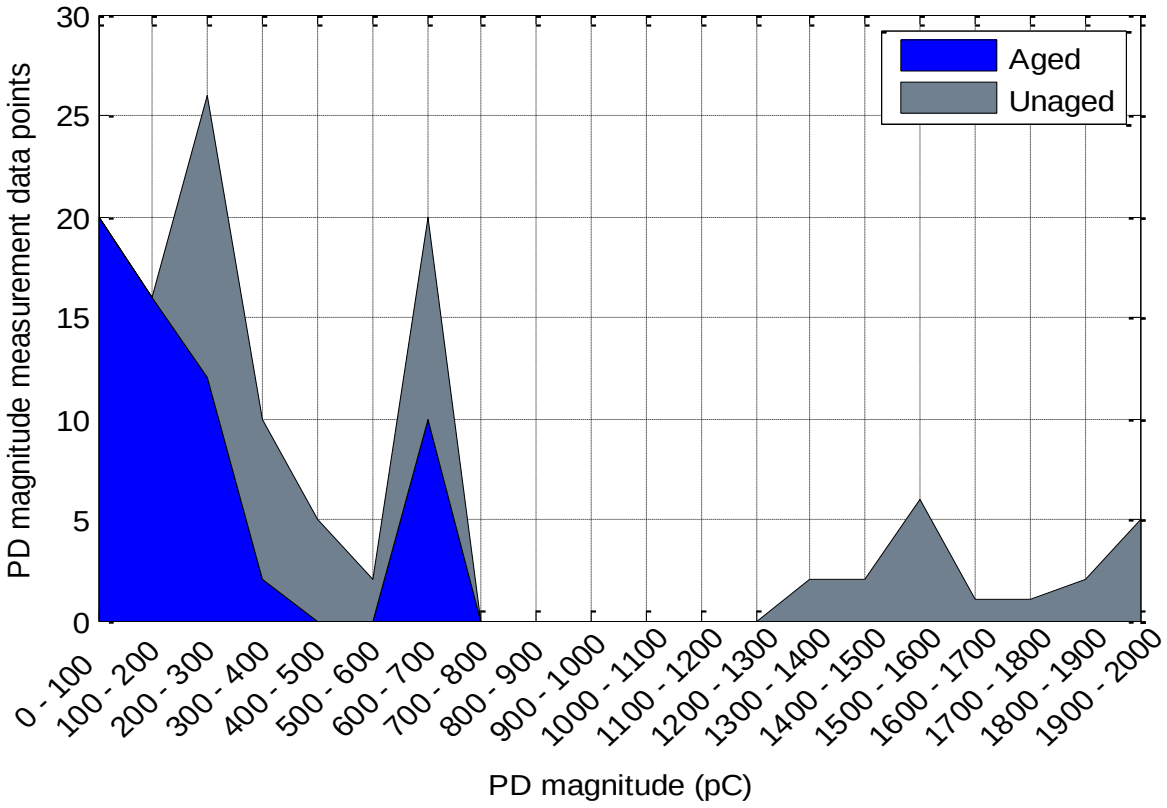

Figure 6-17: Area graph comparing PD magnitude data distribution between un-aged and aged power cable samples

The PD magnitude in of a cylindrical cavity in a coaxial cable is expressed as in Equation 3.10 (Danikas & Adamis, 1997):

$$q = K\varepsilon\varepsilon_0 \left\{ \left(1 + \frac{B}{\sqrt{2ap}}\right) \Omega \; X \left({}^{1}\Big/_{rIn\frac{R_o}{R_i}} \right) \right\} \tag{3.10}$$

Where:

K	is the geometry factor of the enclosed void [dimensionless]
ε	is the permittivity of the insulation [dimensionless]
ε_0	is the known dielectric constant [F/m]
B	is a constant and gas property [Pa.m]
Ω	is the void volume [m^3]
p	is the pressure of the air within the cavity [Pa]
r	is the radial position of the cavity [m]
R_i	is the radius of the conductor semicon dielectric interface[m]
R_o	is the radius of the dielectric ground semicon interface [m]
a	is the radius of the cavity [m]

K is equal to ε_r for a disc-shaped void and the permittivity(ε) of XLPE insulation is 2.3. B = 8.6 (Pa.m)1/2, ε_0 = 8.85 x 10^{-12} . The geometric dimensions of the coaxial cable and enclosed cavity defect are as follows: R_o = 9 mm, Ri = 6 mm, r = 7 mm , a= 1.5 mm and b = 1mm. The air within the cavity defect was assumed to be at atmospheric pressure, p = 101.3 kPa. Substituting these values into Equation 3.10 , yields a PD magnitude of 565 pC. The calculated PD magnitude is less than the average measured PD magnitude of the un-aged test sample by an error margin of 24.36%. Due to the inherent statistical nature of PD phenomena, it is challenging to achieve a perfect match between analytical models and practical measurements.

6.2.2 The effect of impulse ageing on PD magnitude

PD magnitude is a key parameter amongst others in assessing PD progression in insulation. In un-aged cavity defects, scarce initial electrons result in PD inception delay and therefore discharges initiate at bigger gap over-voltages. Scarce electrons are caused by the presence of electronegative oxygen and the high work function of un-aged, smooth polymer surfaces. A high work function implies minimal electron generation especially from deep insulation traps. All these result in intermittent PD occurrences and thus large PD magnitudes. This explains the observed wide scattered PD magnitudes in the un-aged power cable test samples.

During impulse ageing of insulation excited electrons with high energy are generated. These electrons penetrate the bulk insulation causing bond scission and charge trapping centres. The latter enhances charge build up and alters the breakdown characteristics of the test samples. Most importantly, this new source of electrons has implications on PD behaviour. An abundance of initiating electrons implies regular PD occurrence at a lower inception voltage and PD magnitude. This explains lower and more uniform PD magnitudes in impulse-aged power cable test samples. The reduction of PD magnitude with ageing is similar to PD magnitude results obtained by (Grzybowski, 2007) on 15 kV XLPE samples aged with 5000 switching impulses. Most standards on PD diagnosis specify maximum allowable PD. It has been assumed that larger PD magnitudes are associated with more deleterious PD defects. The findings of this work however reveal that PD magnitudes of impulse-aged test samples were generally smaller than that of un-aged test samples, thus smaller PD magnitudes may not always indicate a good insulation condition.

6.3 PD inception voltage results and analysis

The following sub-sections contain PD inception voltage results and discusses the effect of impulse ageing on PD inception voltage.

6.3.1 PD inception results

Ten PDIV measurements were taken for each test sample at a time. These are presented in Table 8-13 and Table 8-14 in the appendix correspondingly for the un-aged and impulse aged sample sets. Scatter

plots of PD inception data of un-aged and impulse-aged sample sets are presented in Figure 6-18 and Figure 6-19 respectively.

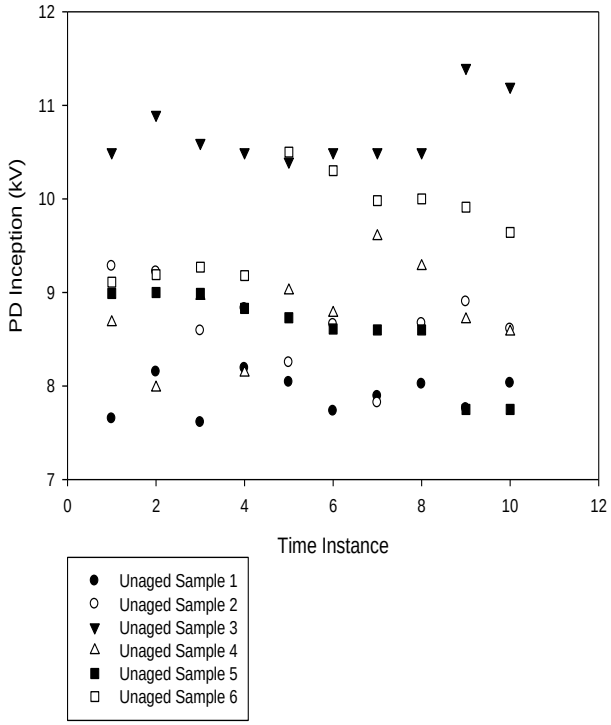

Figure 6-18: PD Inception within un-aged test samples set

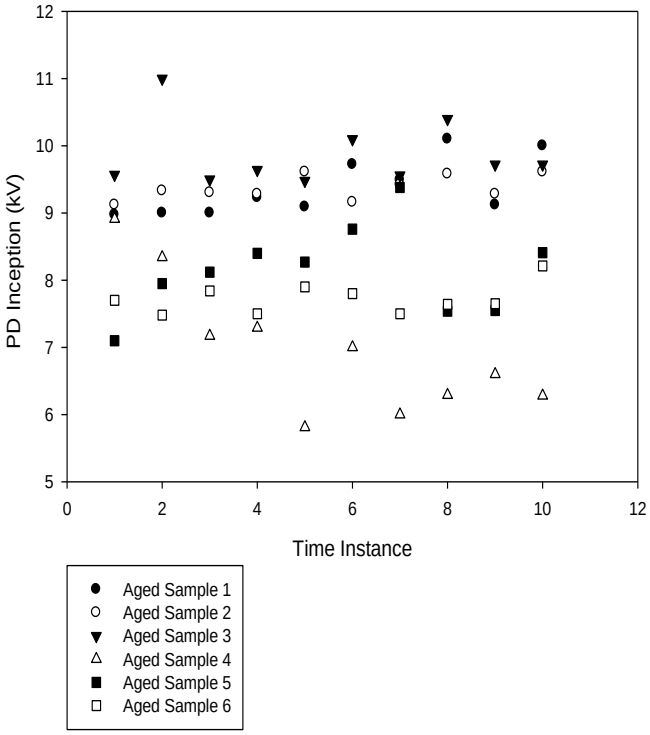

Figure 6-19: PD inception voltage within the aged test sample set

PDIV data range is narrow in both un-aged and impulse-aged power cable test sample sets as illustrated in Figure 6-18 and Figure 6-19 respectively. Furthermore, for a comprehensive picture an average PDIV was calculated for each sample and plotted in Figure 6-20 in order to compare PDIV between un-aged and impulse-aged test samples. Figure 6-20 and Table 6-2.

Table 6-2: PDIV statistical variables of un-aged and impulse-aged power cable test samples

	Mean PD Inception Voltage		Standard Deviation	
	PDIV (kV)	% Difference	Standard deviation	% deviation
Un-aged	9.059	5.64 %	0.995	18%
Aged	8.575		1.178	

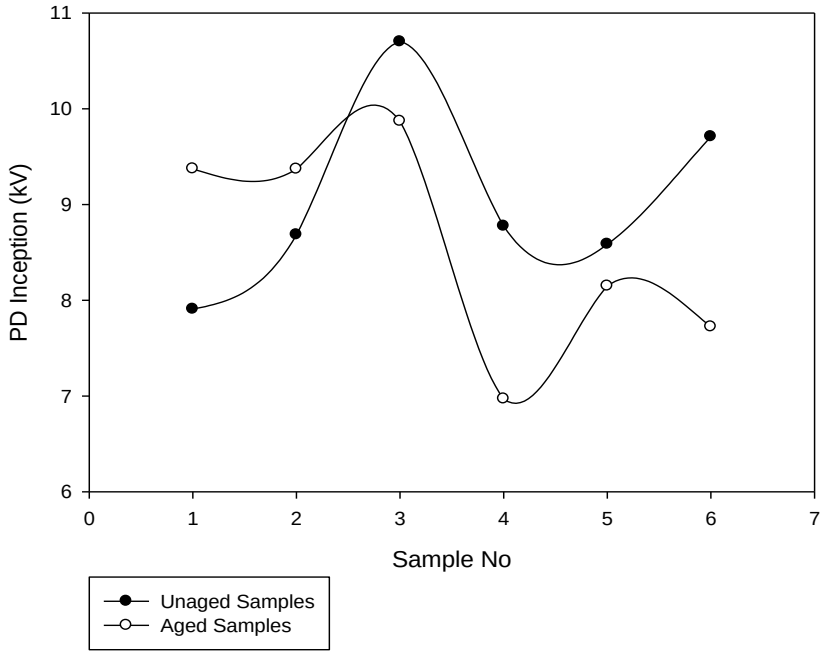

Figure 6-20: Comparison of inception voltage between the un-aged and aged samples

The PDIV standard deviation and arithmetic mean of the aged and un-aged power cable sample sets are within a close magnitude range hence there are close similarities in both. This is supported by Figure 6-18, Figure 6-19 and Figure 6-21.

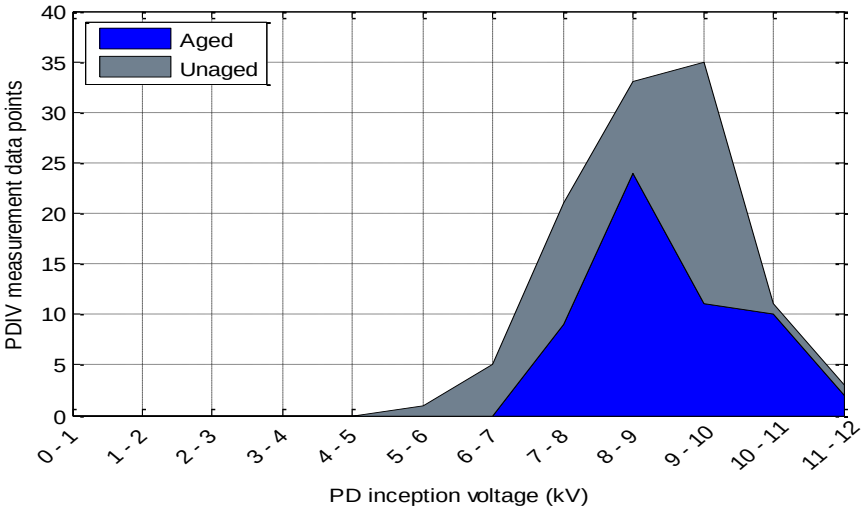

Figure 6-21: Area graph comparing PD magnitude data distribution between un-aged and aged power cable samples

Figure 6-21 shows a graphical presentation of PDIV statistical distribution of un-aged and impulse-aged power cable test samples. The PDIV data distribution of impulse-aged power cable test samples is enveloped by that of un-aged power cable test samples. The distribution range is narrow in both sample sets and indicates coherence.

The PD inception voltage of a coaxial cable insulation is expressed as in (Chan, Duffy, Hiivala, & Wasik, 1991):

$$V_c = 24.2p\left\{rIn\frac{R_o}{R_i}\right\}\left\{\frac{2\varepsilon_r+1}{3\varepsilon_r}\right\}\left\{\frac{8.6}{\sqrt{2ap}}+1\right\} \quad (3.7)$$

Where:

p is the pressure of the air within the cavity [Pa]

r is the radial position of the cavity [m]

R_i is the radius of the conductor semicon dielectric interface[m]

R_o is the radius of the dielectric ground semicon interface [m]

a is the radius of the cavity [m]

ε_r is the relative dielectric constant of the insulation [dimensionless]

The geometric dimensions of the coaxial cable and enclosed cavity defect are as follows: R_o = 9 mm, Ri = 6 mm, r = 7 mm, ε_r = 2.3, a= 1.5 mm and b = 1mm. The air within the cavity is assumed to be at atmospheric pressure, p = 101.3 kPa. Substituting these values into Equation 3.7, yields a PD inception voltage of 8.2 kV. The computed PDIV is less than the measured average PDIV of the un-aged power cable test sample by an error margin of 9.48%. The error is reasonable due to the inherent statistical nature of PD phenomena, it is challenging to achieve a perfect match between analytical models and practical measurements.

6.3.2 The effect of impulse ageing on PD inception voltage

To date no one has actually compared the effect of impulse ageing on PDIV in identical cavity defects used in this research work. The closest work to this dissertation that exists is that by (Zanwar, 2011).

This work however was on inception of PDs caused by impulse surges. The author concluded that it was easier to initiate PDs in impulse aged insulation. However, this cannot be generalized as the experimental methods were different. (Zanwar, 2011) used 15 kV EPR cables and aged them with switching impulses. PD tests were performed at regular intervals during the impulse aging process. Generally PDIV of un-aged power cable test samples was higher than that of impulse-aged test samples although by a small margin. In this case perhaps the lightning stress of 40 kV and number of impulses were not high enough to significantly affect the PD inception voltage. PD theory dictates that un-aged samples would have a higher inception voltage due to the absence of initiating electrons. Aged samples are expected to have a lower PD inception as impulse aging deposits space charge into the insulation. This avails PD initiating electrons and affects the PD mechanism. At this stage the effect of impulse ageing on PD inception is inconclusive.

6.4 Conclusions and pointers to the next chapter

The behaviour of PDs in impulse aged insulation was reviewed by analysis of PD phase resolved patterns, PD magnitude and PD inception. The experimental findings showed that the effect of impulse ageing was more pronounced on PD phase resolved patterns than on PD magnitude and PD inception. Generally, PD magnitude data points of un-aged test samples were higher and less repeatable than that of aged test samples. PD inception voltage of un-aged test samples was marginally higher than that of aged test samples.

7 CONCLUSIONS AND RECOMMENDATIONS

7.1 Key Findings

Literature review reveals that impulse stress affects the electrical and physical properties of polymer insulation and in this research it was hypothesized that this may also have implications on PD behaviour. Experimental work revealed that PD inception, PD magnitude and PDPRP were affected by impulse ageing. PDPRP of un-aged power cable test samples contained a characteristic positive peak PD magnitude that is smaller than the negative peak PD magnitude and a narrower phase angle. The inverse is true in the case of PDPRP of impulse-aged test samples, the negative peak magnitude was either larger or equal to the positive peak magnitude and the phase angle was wider. The effect of impulse ageing of power cable insulation on PD inception voltage was insignificant and it is inconclusive at this stage. Generally, PD magnitude was larger in un-aged power cable test samples and displayed a wide data scatter in comparison with impulse-aged test samples.

7.2 Recommendations for future work

The following are recommended for future work:

- An higher number of lightning impulses
- Dielectric relaxation measurements

An increased number of lightning impulses is suggested with reference to PD inception and perhaps this may affect PD inception. Dielectric relaxation measurements of space charge, permittivity, tan delta and relative permittivity will definitely give a firm indication of what is occurring inside the dielectric physically and this information will provide further insight in the behaviour of PD in impulse aged insulation.

8 APPENDIX

This chapter presents additional figures and tables that were used to measure PDIV and PD magnitude. Ten measurements of PDIV and PD magnitude were taken for each power cable test sample.

8.1 PD Magnitude measurement results

Table 8-1: Measured PDIV of un- aged power cable sample set

Qp Mean [pC]	Qp Mean [pC]	Qp Mean [pC]	Qp Mean [pC]]	Qp Mean [pC]	Qp Mean [pC]
258.67	1527.43	1856.22	639.10	304.52	412.20
263.73	1383.67	1523.22	637.43	306.87	434.08
256.58	1501.93	1883.50	622.57	297.47	504.88
253.84	1473.79	1984.75	617.38	306.86	479.57
282.47	1416.60	1941.30	617.30	303.46	422.00
265.82	1335.34	2003.33	624.06	296.54	251.59
302.13	1538.89	1909.70	633.27	293.24	270.60
266.33	1502.11	1963.70	616.96	309.34	476.67
261.82	1574.40	2067.50	622.80	307.20	366.18
268.81	1619.11	1756.00	611.53	313.44	514.25

Table 8-2: Measured PDIV of aged power cable sample set

Q_p Mean [pC]	Qp Mean [pC]	Qp Mean [pC]	Qp Mean [pC]	Qp Mean [pC]	Qp Mean [pC]
639.10	278.82	90.04	108.27	98.99	26.63
637.43	298.60	87.88	111.93	146.15	21.83
622.57	228.85	82.38	147.94	182.60	34.87
617.38	280.36	89.26	146.69	212.68	34.83
617.30	288.06	94.92	108.85	264.10	27.27
624.06	296.44	92.06	103.36	190.13	22.80
633.27	281.47	103.30	130.83	181.87	17.12
616.96	254.03	101.29	100.99	107.94	22.55
622.80	321.90	99.43	122.18	236.38	24.91
611.53	308.27	94.31	90.01	220.20	44.47

Table 8-3: PD Magnitude measurement results: Un-aged sample 1

Date	Time	Amp In	Sync In	Qp Cur [pC]	Qp Mean [pC]	Qp Max [pC]	Qp Min [pC]	Qp Peak Sup. [pC]	RIV [µV]	U_{rms} [kV]	$U_p/\sqrt{2}$ [kV]	Frequency [Hz]	Aux 1 []	Aux 2 []	ΣQp_i [pC]
02/20/2012	12:08:30	1	1	118.80	116.23	120.30	105.30	118.80	0	12.01	11.91	50.1	-1.000	-1.000	813.60
02/20/2012	12:08:33	1	1	100.80	117.55	124.80	100.80	120.30	0	12.00	11.88	50.1	-1.000	-1.000	705.30
02/20/2012	12:08:36	1	1	124.80	110.46	124.80	85.71	109.80	0	11.98	11.89	50.1	-1.000	-1.000	994.11
02/20/2012	12:08:39	1	1	117.30	117.47	127.80	106.80	117.30	0	12.00	11.88	50.1	-1.000	-1.000	1057.20
02/20/2012	12:08:42	1	1	120.30	119.93	132.30	114.30	118.80	0	11.99	11.89	50.1	-1.000	-1.000	959.40
02/20/2012	12:08:45	1	1	115.80	115.64	127.80	91.73	115.80	0	12.00	11.87	50.1	-1.000	-1.000	1156.43
02/20/2012	12:08:48	1	1	112.80	118.80	130.80	106.80	121.05	0	12.00	11.89	50.1	-1.000	-1.000	950.40
02/20/2012	12:08:51	1	1	126.30	119.74	132.30	106.80	120.30	0	11.99	11.88	50.1	-1.000	-1.000	957.90
02/20/2012	12:08:54	1	1	109.80	118.46	132.30	99.25	118.80	0	12.00	11.88	50.1	-1.000	-1.000	1066.15
02/20/2012	12:08:57	1	1	123.30	120.80	127.80	109.80	123.30	0	11.98	11.88	50.1	-1.000	-1.000	1087.20

Table 8-4: PD Magnitude measurement results: Un-aged sample 2

Date	Time	Amp In	Sync In	Qp Cur [pC]	Qp Mean [pC]	Qp Max [pC]	Qp Min [pC]	Qp Peak Sup. [pC]	RIV [µV]	U_{rms} [kV]	$U_p/\sqrt{2}$ [kV]	Frequency [Hz]	Aux 1 []	Aux 2 []	ΣQp_i [pC]
02/20/2012	12:21:54	1	1	1789.00	1856.22	2075.00	1699.00	1820.00	0	12.13	12.06	50.0	-1.000	-1.000	16706.00
02/20/2012	12:21:57	1	1	1955.00	1523.22	1955.00	481.20	1646.50	0	12.14	12.05	50.0	-1.000	-1.000	15232.20
02/20/2012	12:22:00	1	1	2120.00	1883.50	2120.00	1564.00	1925.00	0	12.14	12.05	50.0	-1.000	-1.000	15068.00
02/20/2012	12:22:03	1	1	1910.00	1984.75	2165.00	1699.00	2067.50	0	12.14	12.06	50.0	-1.000	-1.000	15878.00
02/20/2012	12:22:06	1	1	1940.00	1941.30	2105.00	1639.00	1985.00	0	12.14	12.06	50.0	-1.000	-1.000	19413.00
02/20/2012	12:22:09	1	1	1985.00	2003.33	2150.00	1880.00	2000.00	0	12.13	12.05	50.0	-1.000	-1.000	18030.00
02/20/2012	12:22:12	1	1	1669.00	1909.70	2120.00	1594.00	1955.00	0	12.12	12.04	50.0	-1.000	-1.000	19097.00
02/20/2012	12:22:15	1	1	2165.00	1963.70	2165.00	1684.00	2022.50	0	12.13	12.05	50.0	-1.000	-1.000	19637.00
02/20/2012	12:22:18	1	1	2045.00	2067.50	2180.00	2000.00	2060.00	0	12.12	12.03	50.0	-1.000	-1.000	20675.00
02/20/2012	12:22:21	1	1	1970.00	1756.00	2000.00	1609.00	1669.00	0	12.11	12.06	50.0	-1.000	-1.000	15804.00

Table 8-5: PD Magnitude measurement results: Un-aged sample 3

Date	Time	Amp In	Sync In	Qp Cur [pC]	Qp Mean [pC]	Qp Max [pC]	Qp Min [pC]	Qp Peak Sup. [pC]	RIV [µV]	U_{rms} [kV]	$U_p/\sqrt{2}$ [kV]	Frequency [Hz]	Aux 1 []	Aux 2 []	ΣQp_i [pC]
02/20/2012	12:44:08	1	1	1489.00	1527.43	1789.00	1278.00	1549.00	0	12.08	11.99	49.9	-1.000	-1.000	10692.00
02/20/2012	12:44:11	1	1	1068.00	1383.67	1850.00	1068.00	1414.00	0	12.08	12.01	49.9	-1.000	-1.000	12453.00
02/20/2012	12:44:14	1	1	1805.00	1501.93	1805.00	947.40	1549.00	0	12.08	12.01	49.9	-1.000	-1.000	12015.40
02/20/2012	12:44:17	1	1	1835.00	1473.79	2000.00	932.30	1428.50	0	12.08	11.99	49.9	-1.000	-1.000	11790.30
02/20/2012	12:44:20	1	1	1549.00	1416.60	1835.00	1038.00	1376.00	0	12.09	12.00	49.9	-1.000	-1.000	14166.00
02/20/2012	12:44:23	1	1	1669.00	1335.34	1669.00	541.40	1428.50	0	12.10	12.01	49.9	-1.000	-1.000	13353.40
02/20/2012	12:44:26	1	1	1624.00	1538.89	1835.00	1113.00	1624.00	0	12.10	12.01	49.9	-1.000	-1.000	13850.00
02/20/2012	12:44:29	1	1	1759.00	1502.11	1835.00	1038.00	1564.00	0	12.09	11.99	49.9	-1.000	-1.000	13519.00
02/20/2012	12:44:32	1	1	1880.00	1574.40	1880.00	1053.00	1616.50	0	12.08	11.99	49.9	-1.000	-1.000	15744.00
02/20/2012	12:44:35	1	1	1519.00	1619.11	1940.00	1233.00	1714.00	0	12.08	11.99	49.9	-1.000	-1.000	14572.00

Table 8-6: PD Magnitude measurement results: Un-aged sample 4

Date	Time	Amp In	Sync In	Qp Cur [pC]	Qp Mean [pC]	Qp Max [pC]	Qp Min [pC]	Qp Peak Sup. [pC]	RIV [µV]	U_{rms} [kV]	$U_p/\sqrt{2}$ [kV]	Frequency [Hz]	Aux 1 []	Aux 2 []	ΣQp_i [pC]
02/20/2012	13:04:45	1	1	304.50	304.52	315.80	289.50	304.50	0	12.09	11.99	50.0	-1.000	-1.000	1522.60
02/20/2012	13:04:48	1	1	297.00	306.87	334.60	297.00	306.40	0	12.09	12.01	50.0	-1.000	-1.000	2455.00
02/20/2012	13:04:51	1	1	285.70	297.47	315.80	285.70	297.00	0	12.10	12.00	50.0	-1.000	-1.000	2379.80
02/20/2012	13:04:54	1	1	315.80	306.86	319.50	297.00	304.50	0	12.10	12.01	50.0	-1.000	-1.000	2454.90
02/20/2012	13:04:57	1	1	297.00	303.46	327.10	278.20	297.00	0	12.12	11.99	50.0	-1.000	-1.000	2124.20
02/20/2012	13:05:00	1	1	282.00	296.54	327.10	263.20	297.00	0	12.10	12.01	50.0	-1.000	-1.000	2372.30
02/20/2012	13:05:03	1	1	308.30	293.24	312.00	270.70	295.10	0	12.11	12.01	50.0	-1.000	-1.000	2345.90
02/20/2012	13:05:06	1	1	308.30	309.34	315.80	297.00	312.00	0	12.11	12.01	50.0	-1.000	-1.000	2165.40
02/20/2012	13:05:09	1	1	315.80	307.20	315.80	293.20	308.30	0	12.11	12.01	50.0	-1.000	-1.000	2150.40
02/20/2012	13:05:12	1	1	312.00	313.44	345.90	293.20	306.40	0	12.11	12.00	50.0	-1.000	-1.000	2507.50

Table 8-7: PD Magnitude measurement results: Un-aged sample 5

Date	Time	Amp In	Sync In	Qp Cur [pC]	Qp Mean [pC]	Qp Max [pC]	Qp Min [pC]	Qp Peak Sup. [pC]	RIV [µV]	U_{rms} [kV]	$U_p/\sqrt{2}$ [kV]	Frequency [Hz]	Aux 1 []	Aux 2 []	Σ Qp_i [pC]
02/22/2012	10:34:17	1	1	661.70	639.10	661.70	601.50	654.10	0	12.37	12.22	50.0	-1.000	-1.000	4473.70
02/22/2012	10:34:20	1	1	639.10	637.43	669.20	594.00	646.60	0	12.29	12.14	50.0	-1.000	-1.000	5736.90
02/22/2012	10:34:23	1	1	620.30	622.57	650.40	571.40	624.10	0	11.68	11.53	50.0	-1.000	-1.000	6225.70
02/22/2012	10:34:26	1	1	631.60	617.38	642.90	578.90	620.30	0	11.95	11.81	50.0	-1.000	-1.000	5556.40
02/22/2012	10:34:29	1	1	609.00	617.30	650.40	590.20	616.55	0	12.09	11.94	50.0	-1.000	-1.000	6173.00
02/22/2012	10:34:32	1	1	616.50	624.06	650.40	601.50	624.10	0	12.09	11.93	50.0	-1.000	-1.000	4992.50
02/22/2012	10:34:35	1	1	612.80	633.27	661.70	609.00	635.30	0	12.15	12.01	50.0	-1.000	-1.000	5699.40
02/22/2012	10:34:38	1	1	635.30	616.96	635.30	582.70	612.80	0	12.21	12.08	50.0	-1.000	-1.000	5552.60
02/22/2012	10:34:41	1	1	646.60	622.80	654.10	582.70	620.30	0	12.20	12.05	50.0	-1.000	-1.000	5605.20
02/22/2012	10:34:44	1	1	620.30	611.53	646.60	578.90	605.30	0	12.17	12.02	50.0	-1.000	-1.000	5503.80

Table 8-8: PD Magnitude measurement results: Aged sample 1

Date	Time	Amp In	Sync In	Qp Cur [pC]	Qp Mean [pC]	Qp Max [pC]	Qp Min [pC]	Qp Peak Sup. [pC]	RIV [µV]	U_{rms} [kV]	$U_p/\sqrt{2}$ [kV]	Frequency [Hz]	Aux 1 []	Aux 2 []	Σ Qp_i [pC]
02/22/2012	10:53:46	1	1	233.10	278.82	319.50	233.10	283.80	0	12.09	11.98	50.1	-1.000	-1.000	1672.90
02/22/2012	10:53:49	1	1	278.20	298.60	330.80	263.20	304.50	0	12.09	11.99	50.1	-1.000	-1.000	2090.20
02/22/2012	10:53:52	1	1	210.50	228.85	293.20	188.00	208.65	0	12.09	11.99	50.1	-1.000	-1.000	1830.80
02/22/2012	10:53:55	1	1	176.70	280.36	315.80	176.70	300.80	0	12.10	11.98	50.1	-1.000	-1.000	1962.50
02/22/2012	10:53:58	1	1	266.90	288.06	334.60	199.20	291.35	0	12.09	11.99	50.1	-1.000	-1.000	2304.50
02/22/2012	10:54:01	1	1	330.80	296.44	330.80	210.50	308.30	0	12.11	11.99	50.1	-1.000	-1.000	2075.10
02/22/2012	10:54:04	1	1	293.20	281.47	315.80	195.50	293.20	0	12.08	11.98	50.1	-1.000	-1.000	2251.80
02/22/2012	10:54:07	1	1	282.00	254.03	304.50	206.80	240.60	0	12.09	12.00	50.1	-1.000	-1.000	1778.20
02/22/2012	10:54:10	1	1	308.30	321.90	345.90	293.20	319.55	0	12.08	12.00	50.1	-1.000	-1.000	2575.20
02/22/2012	10:54:13	1	1	304.50	308.27	327.10	293.20	304.50	0	12.09	11.99	50.1	-1.000	-1.000	2157.90

Table 8-9: PD Magnitude measurement results: Aged sample 2

Date	Time	Amp In	Sync In	Qp Cur [pC]	Qp Mean [pC]	Qp Max [pC]	Qp Min [pC]	Qp Peak Sup. [pC]	RIV [µV]	U_{rms} [kV]	$U_p/\sqrt{2}$ [kV]	Frequency [Hz]	Aux 1 []	Aux 2 []	Σ Qp_i [pC]
02/22/2012	11:16:20	1	1	81.20	90.04	118.80	80.45	85.34	0	12.10	12.02	50.0	-1.000	-1.000	720.30
02/22/2012	11:16:23	1	1	70.68	87.88	101.50	69.92	91.73	0	12.10	12.02	50.0	-1.000	-1.000	703.06
02/22/2012	11:16:26	1	1	87.22	82.38	100.00	69.17	84.21	0	12.10	12.02	50.0	-1.000	-1.000	576.69
02/22/2012	11:16:29	1	1	89.47	89.26	91.73	84.21	89.47	0	12.10	12.03	50.0	-1.000	-1.000	624.81
02/22/2012	11:16:32	1	1	106.00	94.92	106.00	87.22	93.99	0	12.11	12.03	50.0	-1.000	-1.000	759.39
02/22/2012	11:16:35	1	1	87.22	92.06	121.10	78.95	87.22	0	12.10	12.03	50.0	-1.000	-1.000	644.45
02/22/2012	11:16:38	1	1	98.50	103.30	112.80	93.23	103.75	0	12.11	12.05	50.0	-1.000	-1.000	826.37
02/22/2012	11:16:41	1	1	93.23	101.29	110.50	93.23	101.50	0	12.10	12.04	50.0	-1.000	-1.000	709.02
02/22/2012	11:16:44	1	1	106.00	99.43	130.80	87.97	94.74	0	12.11	12.03	50.0	-1.000	-1.000	795.44
02/22/2012	11:16:47	1	1	90.23	94.31	104.50	87.22	90.98	0	12.11	12.04	50.0	-1.000	-1.000	660.15

Table 8-10: PD Magnitude measurement results: Aged sample 3

Date	Time	Amp In	Sync In	Qp Cur [pC]	Qp Mean [pC]	Qp Max [pC]	Qp Min [pC]	Qp Peak Sup. [pC]	RIV [µV]	U_{rms} [kV]	$U_p/\sqrt{2}$ [kV]	Frequency [Hz]	Aux 1 []	Aux 2 []	Σ Qp_i [pC]
02/22/2012	11:40:15	1	1	91.73	108.27	219.50	78.20	92.48	0	12.11	12.03	50.0	-1.000	-1.000	866.14
02/22/2012	11:40:18	1	1	171.40	111.93	171.40	93.23	100.80	0	12.11	12.03	50.0	-1.000	-1.000	783.52
02/22/2012	11:40:21	1	1	105.30	147.94	288.70	94.74	113.55	0	12.10	12.03	50.0	-1.000	-1.000	1183.53
02/22/2012	11:40:24	1	1	105.30	146.69	350.00	103.80	118.80	0	12.10	12.02	50.0	-1.000	-1.000	1026.80
02/22/2012	11:40:27	1	1	132.30	108.85	132.30	88.72	104.55	0	12.08	12.01	50.0	-1.000	-1.000	870.76
02/22/2012	11:40:30	1	1	100.80	103.36	111.30	96.24	103.80	0	12.09	12.01	50.0	-1.000	-1.000	723.49
02/22/2012	11:40:33	1	1	87.22	130.83	282.70	87.22	112.80	0	12.09	12.01	50.0	-1.000	-1.000	1046.61
02/22/2012	11:40:36	1	1	97.74	100.99	109.80	90.23	105.30	0	12.08	12.02	50.0	-1.000	-1.000	706.90
02/22/2012	11:40:39	1	1	88.72	122.18	246.60	87.22	100.03	0	12.12	12.01	50.0	-1.000	-1.000	977.44
02/22/2012	11:40:42	1	1	87.22	90.01	99.25	85.71	88.72	0	12.09	12.03	50.0	-1.000	-1.000	630.08

Table 8-11: PD Magnitude measurement results: Aged sample 4

Date	Time	Amp In	Sync In	Qp Cur [pC]	Qp Mean [pC]	Qp Max [pC]	Qp Min [pC]	Qp Peak Sup. [pC]	RIV [µV]	U_{rms} [kV]	$U_p/\sqrt{2}$ [kV]	Frequency [Hz]	Aux 1 []	Aux 2 []	ΣQp_i [pC]
02/22/2012	12:05:38	1	1	82.71	98.99	154.10	82.71	88.35	0	12.12	12.03	50.1	-1.000	-1.000	593.96
02/22/2012	12:05:41	1	1	82.71	146.15	424.80	78.95	82.71	0	12.12	12.05	50.1	-1.000	-1.000	1169.17
02/22/2012	12:05:44	1	1	127.80	182.60	398.50	82.71	135.30	0	12.12	12.03	50.1	-1.000	-1.000	1278.21
02/22/2012	12:05:47	1	1	90.23	212.68	496.20	90.23	120.30	0	12.13	12.02	50.1	-1.000	-1.000	1488.76
02/22/2012	12:05:50	1	1	545.10	264.10	545.10	82.71	227.45	0	12.12	12.02	50.1	-1.000	-1.000	2112.79
02/22/2012	12:05:53	1	1	86.47	190.13	473.70	82.71	86.47	0	12.13	12.05	50.1	-1.000	-1.000	1330.89
02/22/2012	12:05:56	1	1	78.95	181.87	368.40	78.95	101.52	0	12.13	12.03	50.1	-1.000	-1.000	1454.92
02/22/2012	12:05:59	1	1	218.00	107.94	218.00	82.71	90.23	0	12.12	12.03	50.1	-1.000	-1.000	755.60
02/22/2012	12:06:02	1	1	109.00	236.38	537.60	86.47	191.75	0	12.14	12.03	50.1	-1.000	-1.000	1891.07
02/22/2012	12:06:05	1	1	548.90	220.20	548.90	78.95	90.23	0	12.13	12.03	50.1	-1.000	-1.000	1541.42

Table 8-12: PD Magnitude measurement results: Aged sample 5

Date	Time	Amp In	Sync In	Qp Cur [pC]	Qp Mean [pC]	Qp Max [pC]	Qp Min [pC]	Qp Peak Sup. [pC]	RIV [µV]	U_{rms} [kV]	$U_p/\sqrt{2}$ [kV]	Frequency [Hz]	Aux 1 []	Aux 2 []	ΣQp_i [pC]
02/20/2012	12:08:30	1	1	118.80	116.23	120.30	105.30	118.80	0	12.01	11.91	50.1	-1.000	-1.000	813.60
02/20/2012	12:08:33	1	1	100.80	117.55	124.80	100.80	120.30	0	12.00	11.88	50.1	-1.000	-1.000	705.30
02/20/2012	12:08:36	1	1	124.80	110.46	124.80	85.71	109.80	0	11.98	11.89	50.1	-1.000	-1.000	994.11
02/20/2012	12:08:39	1	1	117.30	117.47	127.80	106.80	117.30	0	12.00	11.88	50.1	-1.000	-1.000	1057.20
02/20/2012	12:08:42	1	1	120.30	119.93	132.30	114.30	118.80	0	11.99	11.89	50.1	-1.000	-1.000	959.40
02/20/2012	12:08:45	1	1	115.80	115.64	127.80	91.73	115.80	0	12.00	11.87	50.1	-1.000	-1.000	1156.43
02/20/2012	12:08:48	1	1	112.80	118.80	130.80	106.80	121.05	0	12.00	11.89	50.1	-1.000	-1.000	950.40
02/20/2012	12:08:51	1	1	126.30	119.74	132.30	106.80	120.30	0	11.99	11.88	50.1	-1.000	-1.000	957.90
02/20/2012	12:08:54	1	1	109.80	118.46	132.30	99.25	118.80	0	12.00	11.88	50.1	-1.000	-1.000	1066.15
02/20/2012	12:08:57	1	1	123.30	120.80	127.80	109.80	123.30	0	11.98	11.88	50.1	-1.000	-1.000	1087.20

8.2 PD inception measurements of un-aged power cable samples

Table 8-13: PD inception measurement results of un-aged power cable sample set

Instance	PDIV Sample 1	PDIV Sample 2	PDIV Sample 3	PDIV Sample 4	PDIV Sample 5	PDIV Sample 6
1st	7.65 kV	9.28 kV	9.08 kV	8.68 kV	8.99 kV	9.11 kV
2nd	8.15 kV	9.22 kV	10.50 kV	7.98 kV	9.00 kV	9.19 kV
3rd	7.61 kV	8.59 kV	10.90 kV	8.96 kV	8.99 kV	9.27 kV
4th	8.19 kV	8.83 kV	10.60 kV	8.14 kV	8.83 kV	9.18 kV
5th	8.04 kV	8.25 kV	10.50 kV	9.02 kV	8.73 kV	10.5 kV
6th	7.73 kV	8.66 kV	10.40 kV	8.78 kV	8.61 kV	10.3 kV
7th	7.89 kV	7.82 kV	10.50 kV	9.60 kV	8.60 kV	9.98 kV
8th	8.02 kV	8.67 kV	10.50 kV	9.28 kV	8.60 kV	10.00 kV
9th	7.76 kV	8.90 kV	11.40 kV	8.71 kV	7.75 kV	9.91 kV
10th	8.03 kV	8.61 kV	11.20 kV	8.58 kV	7.75 kV	9.64 kV

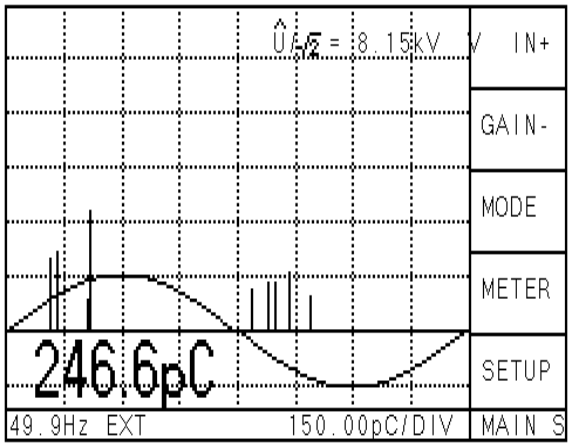

Figure 8-1: PDIV phase resolved pattern un-aged sample 1

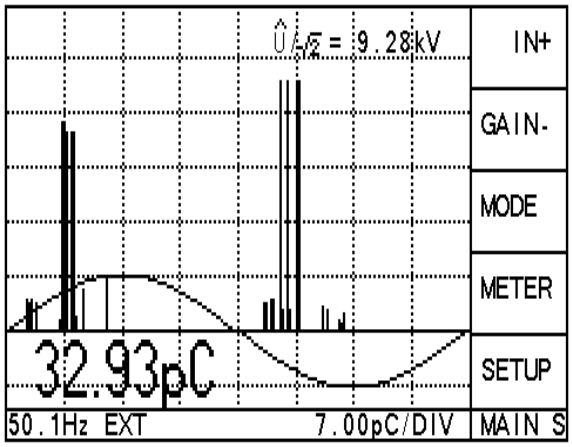

Figure 8-2: PDIV phase resolved pattern un-aged sample 2

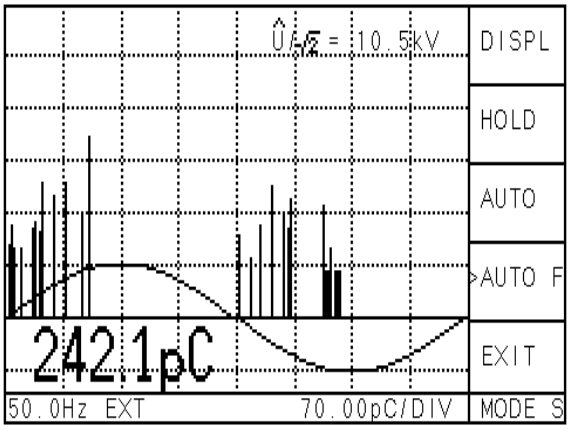

Figure 8-3: PDIV phase resolved pattern un-aged sample 3

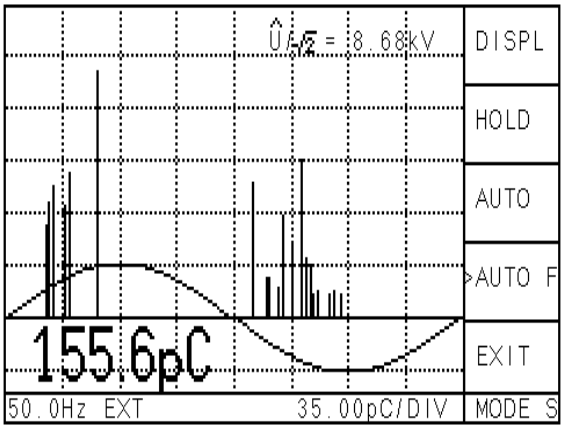

Figure 8-4: PDIV phase resolved pattern un-aged sample 4

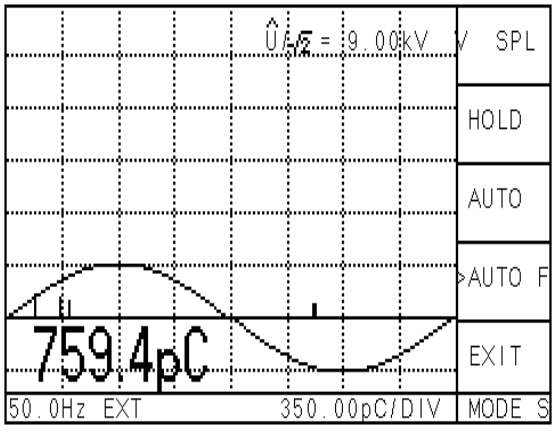

Figure 8-5: PDIV phase resolved pattern un-aged sample 5

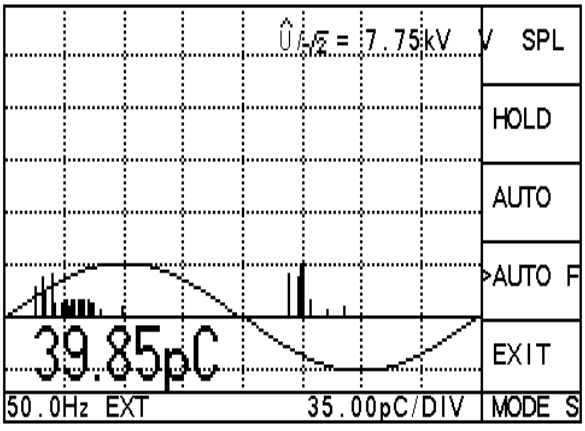

Figure 8-6: PDIV phase resolved pattern un-aged sample 6

8.3 PD inception voltage measurement results of aged power samples

Table 8-14: PD Magnitude measurement results for aged power cable sample set

Instance	PDIV Sample 1	PDIV Sample 2	PDIV Sample 3	PDIV Sample 4	PDIV Sample 5	PDIV Sample 6
1	8.97 kV	9.12 kV	9.57 kV	8.91 kV	7.10 kV	7.70 kV
2	9.00 kV	9.33 kV	11.00 kV	8.34 kV	7.95 kV	7.48 kV
3	9.00 kV	9.30 kV	9.50 kV	7.17 kV	8.12 kV	7.84 kV
4	9.23 kV	9.28 kV	9.64 kV	7.29 kV	8.40 kV	7.50 kV
5	9.09 kV	9.61 kV	9.48 kV	5.81 kV	8.27 kV	7.90 kV
6	9.72 kV	9.16 kV	10.10 kV	7.00 kV	8.76 kV	7.80 kV
7	9.49 kV	9.42 kV	9.56 kV	6.00 kV	9.38 kV	7.50 kV
8	10.10 kV	9.58 kV	10.4 kV	6.29 kV	7.54 kV	7.64 kV
9	9.12 kV	9.28 kV	9.72 kV	6.60 kV	7.55 kV	7.65 kV
10	10.00 kV	9.61 kV	9.72 kV	6.28 kV	8.41 kV	8.21 kV

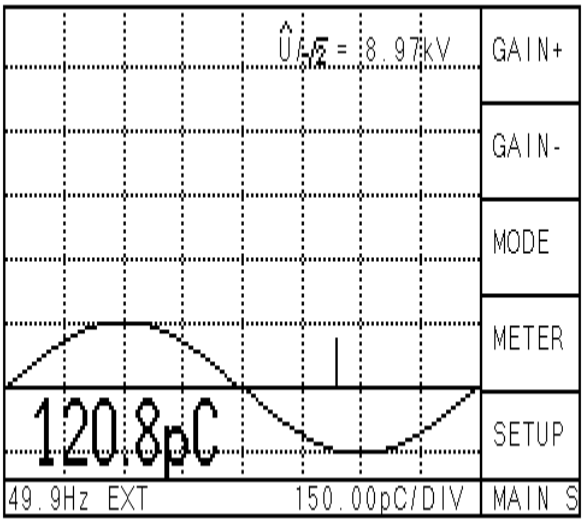

Figure 8-7: PDIV phase resolved pattern aged cable sample 1

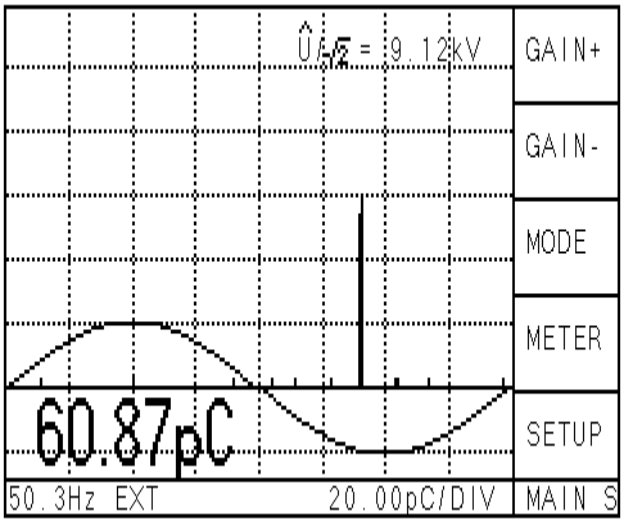

Figure 8-8: PDIV phase resolved pattern aged cable sample 2

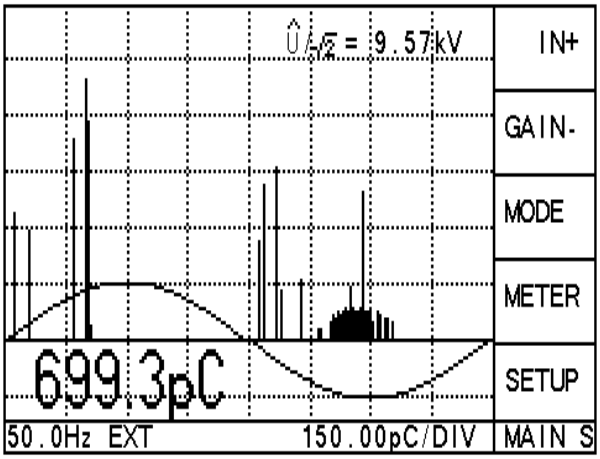

Figure 8-9: PDIV phase resolved pattern aged cable sample 3

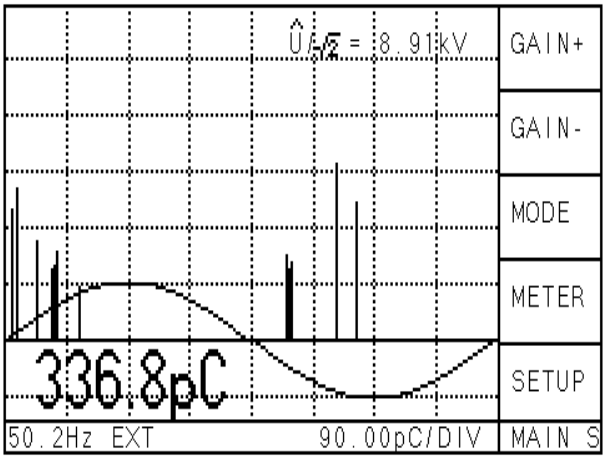

Figure 8-10: PDIV phase resolved pattern aged cable sample 4

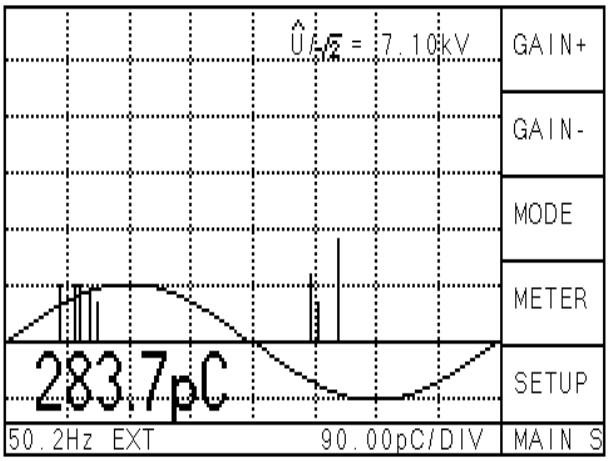

Figure 8-11: PDIV phase resolved pattern aged cable sample 5

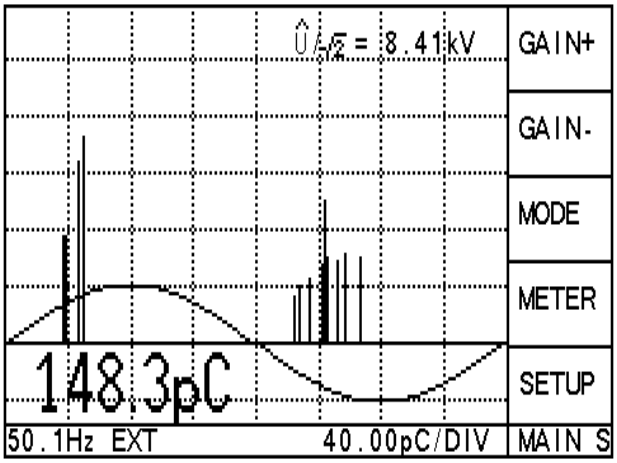

Figure 8-12: PDIV phase resolved pattern aged cable sample 6

9 REFERENCES

Bahaardoorsigh, S., & Rowland, S. M. (2005). The Relationship Between Impulse Ageing and Power Network Performance.

Bartnikas, R. (2002). Partial discharges: Their mechanism, detection and measurement. *IEEE Transactions on Dielectrics and Electrical Insulation, Vol. 9*(No. 5), 763-802.

Berstein, B. S. (2012, April 02). Retrieved April 02, 2012, from IEEE Power and Energy Society ICC Website: http://www.pesicc.org/iccwebsite/subcommittees/subcom_e/E4/2001/f2001_bernstein.pdf

Chan, J. C., Duffy, P., Hiivala, L. J., & Wasik, J. (1991, September/October). Partial Discharge - Part VIII: PD testing of solid dielectric cable. *IEEE Electrical Insulation Magazine, Vol. 7*(No. 5).

Crichton, G. C., Karlsson, P. W., & Pederson, A. (1989, April). Partial discharges in ellipsoidal and spheroidal voids. *IEEE Transactions on Electrical Insulation, Vol. 24*(No. 2), 335-342.

Danikas, M. G., & Adamis, G. (1997). Partial discharges in epoxy resin voids and the interpretational possibilities and limitations of Pedersen's model. *Electrical Engineering*(No. 80), pp. 105 - 110.

Dao, N. L., Lewin, P. L., & Swingler, G. S. (2009). Effect of lightning impulses on the dielectric properties of HDPE. *11th International electrical insulation conference.* Birmingham, UK.

Dao, N. L., Lewin, P. L., & Swingler, S. G. (2009). Lightning impulse ageing of hv cable insulation. *Proceedings of the 16th International Symposium on High voltage engineering.* Cape Town, South Africa.

Densley, R. J., & Salvage, B. (1971). Partial discharges in gaseous cavities in solid dielectrics under impulse voltage conditions. *IEEE Transactions on Electrical Insulation, Vol. E1-6*(No. 2), pp. 54 - 62.

Devins, J. C. (1984). The physics of partial discharges in solid dielectrics. *IEEE Trans. Electr. Insul, Vol. 19*, pp. 475-495.

Fruth, B., & Niemeyer, L. (1992, February). The importance of the statistical characteristics of partial discharge data. *IEEE Transactions on Dielectrics and Electrical Insulation, Vol. 27*(No. 1), 60-69.

Gamez-Garcia, M., Bartnikas, R., & Wertheimer, M. R. (1987). Synthesis reactions involving XLPE subjected to partial discharges. *IEEE Transactions on Electrical Insulation, Vol. E1 - 22*(No. 2), pp. 199 - 205.

Grzybowski, S. (2007). Aging of high vlotage cables by switching impulse. *IEEE Electric Ship Technologies Syposium*, (pp. pp. 165 - 168).

Grzybowski, S., Cao, L., & Shrestha, P. (2009). Electrical degradation of 15 kV XLPE and EPR cable energized by switching impulses. *Proc. of 16th International Symposium on High Voltage Engineering,*. Cape Town, South Africa.

Gulski, E. (1995, October). Digital analysis of partial discharges. *IEEE Transactions on Dielectrics and Electrical Insulation, Vol. 2*(No. 5), pp. 822 - 837.

Gulski, E., Morshuis, P. H., & Kreuger, F. H. (1994). Conventional and Time-resolved measurements of partial discharges as a tool for diagnosis of insulating materials. *Proceedings of the 4th International Conference on Properties and Applications of Dielectric Materials, Vol. 2*, pp. pp. 666-669. Brisbane, Australia.

Gutfleisch, F., & Niemeyer, L. (1995, October). Measurement and simulation of PD in epoxy voids. *IEEE Transactions on Dielectrics and Electrical Insulation, Vol. 2*(No. 5), 729-743.

Hall, J. F. (1993, January). History and bibliography of polymer insulators for outdoor applications. *IEEE Transactions on Power Delivery, Vol. 8*(No. 1), 376 - 385.

Hartlein, R. A., Harper, V. S., & Ng, H. W. (1989). Effects of voltage impulse in extruded dielectric cable life. *IEEE Transactions of Power Delivery, Vol. 4*(No. 2), pp. 829 - 841.

Hudon, C., & Bartnikas, R. (1990, June 3 - 6). Surface conductivity of epocy subjected to partial discharges. *Record of the 1990 IEEE International Symposium on Electrical Insulation*, pp. 153 - 155.

Hudon, C., Bartnikas, R., & Wertheimer, M. R. (1991). Analysis of degradation products on epoxy surfaces subjected to pulse and glow type discharges. *IEEE 91-CH3055-1*, pp. 237 - 243.

Hudon, C., Bartnikas, R., & Wertheimer, M. R. (1993). Spark-to-glow discharge transition due to increased surface conductivity or epoxy resin specimens. *IEEE Transactions on Elelectrical Insulation, Vol. 28,* pp. 1 - 8.

Hudon, C., Bartnikas, R., & Wertheimer, M. R. (1994). Chemical and physical effects on epoxy surfaces exposed to partial discharges. *Proceedings of the 4th International Conference on Properties and Applications of Dielectric Materials,* (pp. 811-814). Brisbane, Australia.

Hudon, C., Bartnikas, R., & Wertheimer, M. R. (1995, December). Effects of physico-chemical degradation of epoxy resin on partial discharge behaviour. *IEEE Transactions on Dielectrics and Electrical Insulation, Vol. 2*(No. 6), pp. 1083 - 1094.

Husain, E., & Nema, R. S. (1982, August). Analysis of Paschen curves for air, N2 and SF6 using the Townsend breakdown mechanism. *IEEE Transactions on Electrical Insulation, Vol. E1-17*(No. 4), 350-353.

IEEE Power Engineering Society. (2006). *IEEE Guide for partial discharge testing of shielded power cable systems in a field environment.* IEEE Std 400.3 TM.

Kao, K. C., & Demin, T. (2003). Hole injection initiated by ionic conduction in electrically stressed insulating polymers. *Journal of Applied Polymer Science, Vol. 90*(No. 7), pp. 1864 - 1867.

Kelen, A. (1995). Trends in PD diagnostics: When new options proliferate, so do old and new problems. *IEEE Transactions on Dielectrics and Electrical Insulation, Vol. 2*(No. 4), pp. 529- 534.

Kreuger, F. H. (1989). *Partial discharge detection in high voltage equipment.* Butterworths & Co.

Kuffel, E., Zaengl, W. S., & Kuffel, J. (2000). *High voltage engineering: Fundementals* (2nd ed.). Butterworth-Heinemann.

Lindell, E., Bengtsson, T., Blennow, J., & Gubanski, S. M. (2008). Measurement of partial discharges at rapidly changing voltages. *IEEE Transactions on Dielectrics and Electrical Insulation, Vol. 15*(N0. 3).

Malinonovski, A. S., Noskov, M. D., Sack, M., & Schwab, A. J. (1998). Simulation of partial discharges and electrical tree growth in solid insulation under ac voltage. *Proceedings of the International Conference in Conduction and Breakdown in Solid Dielectric.* Sweden.

Mason, J. H. (1978). Discharges. *IEEE Trans. Electr. Insul., Vol. 13,* pp. 211-238.

Mason, R., Wilson, M. P., Given, M. J., & Fouracre, R. A. (April 2008). Application of partial discharge monitoring to impulse damaged polymeric insulation. *International conference on condition monitoring and diagnostics.* Beijing, China.

Mayoux, C., & Laurent, C. (1995, August). Contribution of PD to electrical breakdown of solid insulating materials. *IEEE Transactions on Dielectrics and Electrical Insulation, Vol. 2*(No. 4), pp. 641 - 652.

Morshuis, P. H. (1995, October). Assessment of dielectric degradation by Ultrawide-band PD detection. *IEEE Transactions on Dielectrics and Solid Insulation, Vol. 2*(No. 5), pp. 744.

Morshuis, P. H. (2005, October). Degradation of solid dielectrics due to internal partial discharge: Some thoughts on progress made and where to go from now. *IEEE Transactions on Dielectrics and Electrical Insulation, Vol. 12*(No. 12), 905-913.

Morshuis, P. H., & Kreuger, H. F. (1990). Transition from streamer to Townsend mechanisms in dielectric voids. *Journal of Applied Physics, Vol. 23*, 1562-1568.

Murata, Y., Katakai, S., & Kanaoka, M. (1996). Impulse breakdown superposed on AC voltage in XLPE insulation. *IEEE Transactions on Dielectrics and Electrical Insulation, Vol. 3*(No. 3), pp. 361 - 365.

Nattrass, D. A. (1993). Partial Discharge XVII: The early history of partial discharge research. *IEEE Electrical Insulation Magazine, Vol. 9*(No. 4), pp. 27 - 31.

Niemeyer, L. (1995, August). A generalized approach to partial discharge modelling. *IEEE Transactions on Dielectrics and Electrical Insulation, Vol. 2*(No. 2), 510-527.

Nyamupangedengu, C. (2011). *PD-Type dependent type spectral bandwidth in solid polymer dielectrics.* PhD-Thesis, University of the Witwatersrand, Johannesburg.

Nyamupangedengu, C., & Jandrell, I. R. (2007). Sizing of artificial PD defects for an accelerated ageing test of a power cable solid dielectric insulation. *South African University Power Engineering Conference.* Capetown, South Africa.

Paoletti, G. J., & Golubev, A. (2001). Partial Discharge Theory and Technologies Related to Medium-Voltage Electrical Equipment. *IEEE TRANSACTIONS ON INDUSTRY APPLICATIONS, Vol. 37*(No. 1), pp. 90 - 103.

SABS-IEC60270. (2001). *High-voltage test techniques - Partial discharge measurements.* Pretoria: SABS.

Sun, Z., Zhao, X., Li, J., & Li, Y. (2009). Comparing investigation of partial discharge under AC, DC and impulse voltage. *Proceedings of the 16th International Symposium on High Voltage Engineering* (pp. pp. 1 - 6). Cape Town: SAIEE.

Swafield, D. J., Lewin, P. L., Dao, N. L., & Hallstroom, J. K. (2007). Lightning impulse wave-shape: defining the true origin and its impact on parameter evaluation. Ljubljana, Slovenia.

Tanaka, T. (1986, December). Internal partial discharge and material degradation. *IEEE Transactions on Electrical Insulation, Vol. E1-21*(No. 6), pp. 899-905.

Temmen, K. (2000). Evaluation of surface changes in flat cavities due to ageing by means of phase-angle resolved partial discharge measurement. *J. Phys. D. Appl. Phys., Vol. 33*, pp. 603-608.

Wang, L., Cavallini, A., & Montanari, G. C. (2012). Evolution of PD patterns in polyethylene insulation cavities under ac voltage. *Vol. 19*(No. 2).

Wetzer, J. M., Pemen, A. J., & van der Laan, P. L. (1991). Experimental study of the mechanism of partial discharge in voids in polyethylene. *Proceedings of the 7th International Symposium on High Voltage.* Dresden.

Wu et al. (2005, December). Contribution of surface conductivity to the current forms of partial discharges in voids. *IEEE Transactions on Dielectrics and Electrical Insulation, Vol. 12*(No. 6), pp. 1116 -1124.

Yilmaz, G. H., Oztas, H., & Kalenderi, O. (1995). A study on testing of heated power cables at impulse voltage. *9th International Syposium on High voltage engineering.* Graz, Austria.

Zanwar, A. U. (2011). *Electrical aging of 15 kV EPR cables energized by ac voltage with switching impulses superimposed.* Mississippi State University, Department of Electrical and Computer Engineering. UMI Dissertation Publishing.